

ปฏิกิริยาไฮโดรจีเนชันบางส่วนของฟีนอลอะเซทิลีนเป็นสไตรีนในวัฏภาคของเหลวบนตัวเร่งปฏิกิริยา
แพลเลเดียมบนไทเทเนียมในคาร์บอนไดออกไซด์วิกฤตยิ่งยวด



นางสาวสุชุมาล สิงชัย

ศูนย์วิทยพัทยาการ

วิทยานิพนธ์นี้เป็นส่วนหนึ่งของการศึกษาตามหลักสูตรปริญญาวิศวกรรมศาสตรมหาบัณฑิต

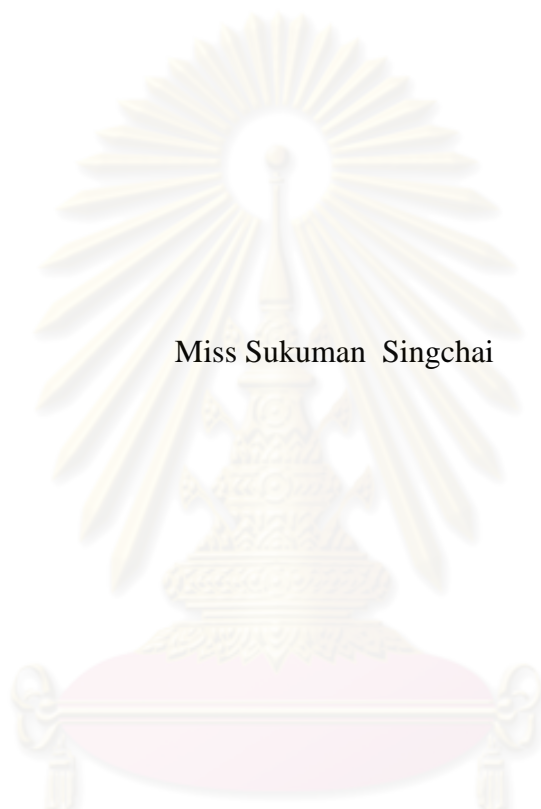
สาขาวิชาวิศวกรรมเคมี ภาควิชาวิศวกรรมเคมี

คณะวิศวกรรมศาสตร์ จุฬาลงกรณ์มหาวิทยาลัย

ปีการศึกษา 2551

ลิขสิทธิ์ของจุฬาลงกรณ์มหาวิทยาลัย

**LIQUID PHASE SEMIHYDROGENATION OF PHENYLACETYLENE TO
STYRENE ON Pd/TiO₂ IN SUPERCRITICAL CARBON DIOXIDE**



Miss Sukuman Singchai

ศูนย์วิทยทรัพยากร
จุฬาลงกรณ์มหาวิทยาลัย

A Thesis Submitted in Partial Fulfillment of the Requirements
for the Degree of Master of Engineering Program in Chemical Engineering

Department of Chemical Engineering

Faculty of Engineering

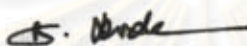
Chulalongkorn University

Academic Year 2008

Copyright of Chulalongkorn University


Thesis Title LIQUID PHASE SEMIHYDROGENATION OF
 PHENYLACETYLENE TO STYRENE ON Pd/TiO₂ IN
 SUPERCRITICAL CARBON DIOXIDE
By Miss Sukuman Singchai
Field of Study Chemical Engineering
Advisor Assistant Professor Joongjai Panpranot, Ph.D.


Accepted by the Faculty of Engineering, Chulalongkorn University in Partial
Fulfillment of the Requirements for the Master's Degree


.....Dean of the Faculty of Engineering
(Associate Professor Boonsom Lerdhirunwong, Dr.Ing.)

THESIS COMMITTEE


.....Chairman
(Associate Professor Paisan Kittisupakorn, Ph.D.)


.....Thesis Advisor
(Assistant Professor Joongjai Panpranot, Ph.D.)


.....Examiner
(Akawat Sirisuk, Ph.D.)


.....External Examiner
(Assistant Professor Okorn Mekasuwandumrong, D.Eng.)

สุชมาล สิงชัย: ปฏิกริยาไฮโดรจิเนชันบางส่วนของฟีนิลอะเซทิลีนเป็นสไตรีนในวัฏภาคของเหลวบนตัวเร่งปฏิกริยาแพลเลเดียมบนไทเทเนียในคาร์บอนไดออกไซด์วิกฤติยิ่งยวด (LIQUID PHASE SEMIHYDROGENATION OF PHENYLACETYLENE TO STYRENE ON Pd/TiO₂ IN SUPERCRITICAL CARBON DIOXIDE) อ. ที่ปริกษาวิทยานิพนธ์หลัก: ผศ. ดร. จุใจ บั้นประณต, 83 หน้า

ในงานวิจัยนี้ได้ทำการศึกษาปฏิกริยาไฮโดรจิเนชันแบบเลือกเกิดในวัฏภาคของเหลวของฟีนิลอะเซทิลีนบนตัวเร่งปฏิกริยาแพลเลเดียมบนตัวรองรับไทเทเนียในคาร์บอนไดออกไซด์วิกฤติยิ่งยวดและเปรียบเทียบในตัวทำละลายอินทรีย์ (เอทานอล) และไม่ใช่ตัวทำละลาย พบว่าอัตราการเกิดปฏิกริยาไฮโดรจิเนชันเพิ่มขึ้นตามลำดับดังนี้ เอทานอลและคาร์บอนไดออกไซด์วิกฤติยิ่งยวด เอทานอล ไม่ใช่ตัวทำละลายและคาร์บอนไดออกไซด์วิกฤติยิ่งยวด ทั้งนี้คาดว่าก๊าซคาร์บอนไดออกไซด์จะเพิ่มความสามารถการละลายของก๊าซไฮโดรเจนในฟีนิลอะเซทิลีนเป็นผลให้ความว่องไวในการเกิดปฏิกริยาไฮโดรจิเนชันเพิ่มขึ้น แต่ในทางตรงกันข้ามการผสมกันระหว่างเอทานอลและคาร์บอนไดออกไซด์วิกฤติยิ่งยวดอาจจะทำให้เกิดของผสมสองวัฏภาคส่งผลให้ความว่องไวของตัวเร่งปฏิกริยาลดต่ำลง นอกจากนี้ยังพบว่าขนาดโลหะแพลเลเดียมไม่ส่งผลต่อความว่องไวเฉพาะสำหรับปฏิกริยาไฮโดรจิเนชันบางส่วนของฟีนิลอะเซทิลีนในคาร์บอนไดออกไซด์วิกฤติยิ่งยวด แต่ในเอทานอลแสดงลักษณะของปฏิกริยาที่ขึ้นกับโครงสร้างของโลหะ โดยค่าความว่องไวเฉพาะของแพลเลเดียมเพิ่มขึ้นเมื่อขนาดโลหะแพลเลเดียมเพิ่มขึ้นเมื่อรีดิวซ์ที่อุณหภูมิ 500 องศาเซลเซียสพบว่าไทเทเนียขนาดใหญ่จะเกิดการหลอมรวมกันของโลหะแพลเลเดียมและไทเทเนียรูคโคที่ขนาดเล็กจะเกิดการเปลี่ยนเฟส ส่งผลให้การกระจายตัวของโลหะแพลเลเดียมและความว่องไวในการเกิดปฏิกริยาไฮโดรจิเนชันลดลง ในขณะที่ตัวเร่งปฏิกริยาบนตัวรองรับไทเทเนียที่เตรียมโดยวิธีโซลโวลเทอรัมอลจะปรากฏอันตรกิริยาระหว่างโลหะแพลเลเดียมและไทเทเนียซึ่งส่งผลในการเพิ่มประสิทธิภาพการเร่งปฏิกริยาไฮโดรจิเนชันแบบเลือกเกิดของฟีนิลอะเซทิลีนโดยทำให้ค่าการเลือกเกิดเป็นผลิตภัณฑ์ที่ต้องการคือสไตรีนสูงขึ้นที่ค่าการแปดผันของฟีนิลอะเซทิลีน 100% ในคาร์บอนไดออกไซด์

ศูนย์วิทยทรัพยากร จุฬาลงกรณ์มหาวิทยาลัย

ภาควิชา.....วิศวกรรมเคมี.....ลายมือชื่อนิสิต..... สุชมาล สิงชัย.....
 สาขาวิชา.....วิศวกรรมเคมี.....ลายมือชื่อ อ. ที่ปริกษาวิทยานิพนธ์หลัก..... ดร. จุใจ บั้นประณต.....
 ปีการศึกษา.....2551.....

5070490721: MAJOR CHEMICAL ENGINEERING

KEYWORDS: LIQUID-PHASE SEMIHYDROGENATION/ SUPER CRITICAL
CARBON DIOXIDE/SMSI

SUKUMAN SINGCHAI: LIQUID PHASE SEMIHYDROGENATION OF
PHENYLACETYLENE TO STYRENE ON Pd/TiO₂ IN SUPERCRITICAL
CARBON DIOXIDE. ADVISOR: ASST. PROF. JOONGJAI PANPRANOT
Ph.D., 83 pp.

In this thesis, liquid-phase selective hydrogenation of phenylacetylene over Pd/TiO₂ has been studied in supercritical carbon dioxide (scCO₂) and compared to that in organic solvent (ethanol) and solventless condition. It was observed that hydrogenation rate increased in the order: scCO₂ > solventless > ethanol > ethanol+scCO₂. The H₂ solubility in phenylacetylene may be enhanced by dissolution of CO₂ resulting in an increase in hydrogenation activity. On the other hand, the mixture of ethanol and scCO₂ may lead to a biphasic reaction mixture so that lower catalytic activity was obtained. The Pd particle size did not affect specific activity for semihydrogenation of phenylacetylene in scCO₂ but in ethanol, the reaction appeared to be structure sensitive since the TOF increase with an increase in Pd particles size. Reduction at high temperature (500°C) caused metal sintering and TiO₂ phase change for micron-size anatase TiO₂ and nano-size brookite TiO₂, respectively. As a consequence, lower Pd dispersion and lower hydrogenation activity were obtained over these catalysts. On the other hand, the use of solvothermal-derived TiO₂ supported catalyst exhibited the strong metal-support interaction effect which improved the catalyst performance especially when the conversion of phenylacetylene was nearly completed in scCO₂.

ศูนย์วิจัยทรัพยากร
จุฬาลงกรณ์มหาวิทยาลัย

Department :..... Chemical Engineering

Field of Study :..... Chemical Engineering

Academic Year :2008.....

Student's Signature :..... Sukuman Singchai

Advisor's Signature :..... J. Pan

ACKNOWLEDGEMENTS

The author would like to express his sincere gratitude and appreciation to her advisor, Assistant Professor Joongjai Panpranot, for her invaluable suggestions, encouragement during her study, and useful discussion throughout this research. In addition, the author would also be grateful to Associate Professor Paisan Kittisupakorn, as the chairman, Dr. Akawat Sirisuk and Assistant Professor Okorn Mekasuwandumrong as the members of the thesis committee.

Most of all, the author would like to express her highest gratitude to her parents who always pay attention to her all the times for their suggestions and have provided support and encouragements. The most success of graduation is devoted to her parents.

Moreover, the author wishes to thank the members of the Center of Excellence on Catalysis and Catalytic Reaction Engineering, Department of Chemical Engineering, Faculty of Engineering, Chulalongkorn University. To the many others, not specifically named, who have provided her with support and encouragement, please be assured that she thinks of you.

Finally, the author would like to thank the Thailand Research Fund (TRF), as well as the Graduate School of Chulalongkorn University for their financial supports.

ศูนย์วิทยทรัพยากร
จุฬาลงกรณ์มหาวิทยาลัย

CONTENTS

	page
ABSTRACT (THAI)	iv
ABSTRACT (ENGLISH)	v
ACKNOWLEDGMENTS	vi
CONTENTS	vii
LIST OF TABLES	x
LIST OF FIGURES	xi
CHAPTER	
I INTRODUCTION	1
1.1 Rationale.....	1
1.2 Research Objectives.....	2
1.3 Research Scopes.....	2
1.4 Research Methodology.....	4
II THEORY	5
2.1 Selective Hydrogenation Reaction of Alkynes to Alkene.....	5
2.2 Physico-Chemical Properties of Supercritical Carbon Dioxide...	7
2.3 Palladium.....	9
2.4 Titanium (IV) oxide	10
III LITERATURE REVIEWS	15
3.1 Synthesis of nanocrystalline TiO ₂ by solvothermal method	15
3.2 Supported Pd catalyst in liquid-phase hydrogenation	16
3.3 Role of TiO ₂ in selective hydrogenation	17
3.4 Liquid phase hydrogenation in supercritical carbon dioxide.....	18
3.5 Comments on the previous works	20
IV EXPERIMENTAL	21
4.1 Catalyst Preparation	21
4.1.1 Praperation of TiO ₂ supports using solvothermal method	21
4.1.2 Palladium Loading	23
4.2 The Reaction Study in Liquid-Phase Hydrogenation	23
4.2.1 Chemicals and Reagents	23

CHAPTER	page
4.2.2 Instruments and Apparatus	24
4.2.3 Liquid-Phase Hydrogenation Procedure	25
4.3 Catalyst Characterization	26
4.3.1 X-ray Diffraction (XRD).....	26
4.3.2 N ₂ Physisorption	26
4.3.3 Transmission Electron Microscopy (TEM).....	27
4.3.4 Scanning Electron Microscopy (SEM).....	27
4.3.5 CO-Pulse Chemisorption	27
4.3.6 Electron Spin Resonance (ESR).....	28
V RESULTS AND DISCUSSION	29
5.1 Characterization of TiO ₂ supports and Pd/TiO ₂ catalysts.....	29
5.1.1 X-Ray Diffraction (XRD).....	29
5.1.2 N ₂ Physisorption.....	34
5.1.3 Scanning Electron Microscopy (SEM).....	36
5.1.4 Transmission Electron Microscopy (TEM).....	43
5.1.5 Metal active sites.....	50
5.1.6 Strong Metal Support Interaction Test.....	51
5.1.7 Electron Spin Resonance (ESR).....	53
5.2 Reaction study in phenylacetylene hydrogenation.....	55
5.2.1 Comparison of organic solvent and scCO ₂ in semihydrogenation of phenylacetylene on 1%Pd/TiO ₂ -An catalyst.....	55
5.2.2 Influence of CO ₂ pressure and reaction time on the catalytic behavior of different 1%Pd/TiO ₂ catalysts in semihydrogenation of phenylacetylene.....	56
5.2.3 Effect of Pd ⁰ metal particle size on semihydrogenation of phenylacetylene in organic solvent and scCO ₂	62

	page
CHAPTER	
VI CONCLUSIONS AND RECOMMENDATIONS.....	67
6.1 Conclusions.....	67
6.2 Recommendations.....	68
REFERENCES.....	69
APPENDICES	
APPENDIX A. CALCULATION FOR CATALYST PREPARATION.....	74
APPENDIX B. CALCULATION OF THE CRYSTALLITE SIZE.....	75
APPENDIX C. CALCULATION FOR METAL ACTIVE SITES AND DISPERSION.....	78
APPENDIX D. CALCULATION OF PHENYLACETYLENE CONVERSION AND SELECTIVITY.....	80
APPENDIX E. CALCULATION OF TURNOVER OF FREQUENCY	81
APPENDIX F. LIST OF PUBLICATIONS.....	82
VITAE.....	83

ศูนย์วิทยทรัพยากร
จุฬาลงกรณ์มหาวิทยาลัย

LIST OF TABLES

TABLE	Page
2.1 Physical properties of palladium.....	9
2.2 Crystallographic properties of anatase, brookite, and rutile	11
4.1 Chemicals used in the preparation of TiO ₂	21
4.2 The condition used for the preparation of TiO ₂	22
4.3 The chemicals and reagents used in the reaction.....	23
4.4 Operating conditions for the GC-MS	24
5.1 The crystallite sizes and phase composition of TiO ₂ support and 1%Pd/TiO ₂ catalysts	32
5.2 N ₂ physisorption properties of TiO ₂ supports and Pd supported on TiO ₂ catalysts	35
5.3 The crystallite sizes of difference TiO ₂ support.....	43
5.4 Results from CO chemisorption of Pd supported on TiO ₂ catalysts	51
5.5 Semihydrogenation of phenylacetylene on 1%Pd/TiO ₂ -An catalysts...	56
5.6 Catalytic activity of defferent 1%Pd/TiO ₂ catalysts in semihydrogynation of phenylactylene in ethanol at 303 K	64
5.7 Previous studies reporting the effect of Pd ⁰ metal particle size in selective hydrogenation reaction in which larger Pd ⁰ particle size was found to be more activity.....	66

ศูนย์วิทยทรัพยากร
 จุฬาลงกรณ์มหาวิทยาลัย

LIST OF FIGURES

FIGURE	Page
1.1 Flow diagram of research methodology	4
2.1 Scheme of Phenylacetylene hydrogenation	7
2.2 Schematic phase diagram of carbon dioxide	8
2.3 Crystal structure of TiO ₂	12
4.1 The schematic drawing of equipments used for the preparation of TiO ₂	22
4.2 The schematic diagram of liquid-phase hydrogenation	26
5.1 The XRD patterns of the TiO ₂ polymorphs	31
5.2 The XRD patterns of 1%Pd/TiO ₂ when reduced at 40°C	33
5.3 The XRD patterns of 1%Pd/TiO ₂ when reduced at 500°C	33
5.4 SEM micrographs of TiO ₂ supports and Pd supported on TiO ₂ catalysts	42
5.5 TEM micrographs of TiO ₂ supports and Pd supported on TiO ₂ catalysts	49
5.6 The results of SMSI test on 1%Pd/TiO ₂ catalysts	52
5.7 ESR spectra of TiO ₂	54
5.8 Influence of CO ₂ pressure on semihydrogenation of phenylacetylene on 1%Pd/TiO ₂ -An catalyst.....	57
5.9 Influence of reaction time on semihydrogenation of phenylacetylene	58
5.10 Influence of CO ₂ pressure on semihydrogenation of phenylacetylene on 1%Pd/TiO ₂ -An and 1%Pd/TiO ₂ -Br catalysts.....	60
5.11 Performance curve of 1%Pd/TiO ₂ An and SV.....	61
5.12 Influence of metal particle size on the overall conversion of phenylacetylene and selectivity to styrene for 1%Pd/TiO ₂ -R40 in organic solvent and scCO ₂	63
5.13 Plot TOF against metal particle size for semihydrogenation of phenylacetylene in ethanol	65
B.1 The measured peak of TiO ₂ -micron for calculation the crystallite size.....	77

FIGURE**Page**

- B.2 The plot indicating the value of line broadening due to the equipment.
The data were obtained by using α -alumina as standard..... 77



ศูนย์วิทยทรัพยากร
จุฬาลงกรณ์มหาวิทยาลัย

CHAPTER I

INTRODUCTION

1.1 Rationale

Semihydrogenation of phenylacetylene is a reaction of industrial importance. This compound is an unwanted feedstock component in polystyrene production plants, and its removal to levels below 10 ppm is mandatory to avoid poisoning of the polymerization catalyst (S. D. Domínguez et al, 2008). Furthermore, semihydrogenation of phenylacetylene is a very convenient process for catalyst optimization, because it enables both evaluation of process design (T. Vergunst et al, 2001) and quick testing of hydrogenation catalysts (X. Huang et al, 2003) under very mild conditions.

Hydrogenation reactions are mostly catalyzed by noble metals or group VIII transition metals because they adsorb hydrogen with dissociation and the bonding is not too strong. The major advantages of noble metal catalysts are their relatively high activity, mild process conditions, easy separation, and better handling properties. The noble metals which have an effective in hydrogenation process are Pd, Pt, Rh, and Ru. However, supported Pd-based catalyst is known to be the best catalyst so far for such reaction with good activity and selectivity. Generally, the catalyst support must present a good stability to high temperature and a sufficiently large specific surface area. Silica (U. K. Singh et al, 2001), alumina (M. Burgener et al, 2004), MCM-14 (S. D. Domínguez et al, 2008) and titania (P. Weerachawansak et al, 2008) have been used in preparation of supported palladium catalyst for selective hydrogenation in liquid phase but titania was selected as a candidate support catalysts because it is well-known that it interacts strongly with Pd, particularly after reduction at high temperatures. The phenomenon is referred to as “the strong metal-support interaction” (SMSI) and has been observed with catalysts supported on reducible metal oxides, including titania (S. J. Tauster et al, 1978).

The rate of catalytic hydrogenation in a gas liquid system is not so high and one reason for this is a small solubility of gaseous hydrogen in common solvents.

In contrast, hydrogen is completely miscible with supercritical carbon dioxide (scCO₂). When all other reacting species and catalysts are also soluble in scCO₂, mass transfer problems can be avoided (F. Zhao et al, 2002). Moreover, the use of scCO₂ as a new clean reaction medium to replace conventional organic solvents, because it is nontoxic, inexpensive, nonflammable and enable easy separation of the solvents from the reactants and products (R. Liu et al, 2007). Bhanage and coworkers (B. M. Bhanage et al, 1999) found that the hydrogenation of α, β -unsaturated aldehydes could be performed successfully in scCO₂ with a significant improvement in activity and product selectivity. The selectivity of unsaturated alcohols depends mainly on pressure of carbon dioxide while the conversion depends on both carbon dioxide and hydrogen pressures.

In this thesis, liquid-phase hydrogenation of phenylacetylene over Pd/TiO₂ has been studied under pressurized carbon dioxide and compared to that in organic solvent or the mixture of organic solvent and carbon dioxide. The physicochemical properties of the catalysts were also investigated by means of N₂ physisorption, X-ray diffraction (XRD), CO-temperature programmed desorption (CO-TPD), CO pulse chemisorption, electron spin resonance (ESR) and transmission electron microscopy (TEM).

1.2 Research Objectives

The objective of this research is to investigate the effect of pressurized CO₂ on the catalytic properties of TiO₂ supported Pd catalysts in liquid-phase selective hydrogenation of phenylacetylene to styrene.

1.3 Research Scopes

1. Preparation of 1%Pd/TiO₂ catalysts using incipient wetness impregnation method on different TiO₂ supports as follows:
 - Anatase TiO₂ - from Aldrich
 - Anatase TiO₂ - prepared by solvolthematic method
 - Rutile TiO₂ - from Aldrich

Brookite TiO₂ - prepared by school of Material science and Engineering,
Clemson University

2. Reduction of Pd/TiO₂ catalyst at 40 and 500°C
3. Characterization of the catalysts and catalyst supports using several techniques such as, X-ray diffraction (XRD), N₂ physisorption, Transmission electron microscopy (TEM), CO pulse chemisorption, and electron spin resonance (ESR).
4. Reaction study in liquid-phase selective hydrogenation of phenylacetylene on Pd/TiO₂ in various reaction media as follows:
 - CO₂
 - Ethanol
 - Solventless
 - CO₂+Ethanol

CO₂ pressure is varied in the range of 0-16 MPa



ศูนย์วิทยทรัพยากร
จุฬาลงกรณ์มหาวิทยาลัย

1.4 Research Methodology

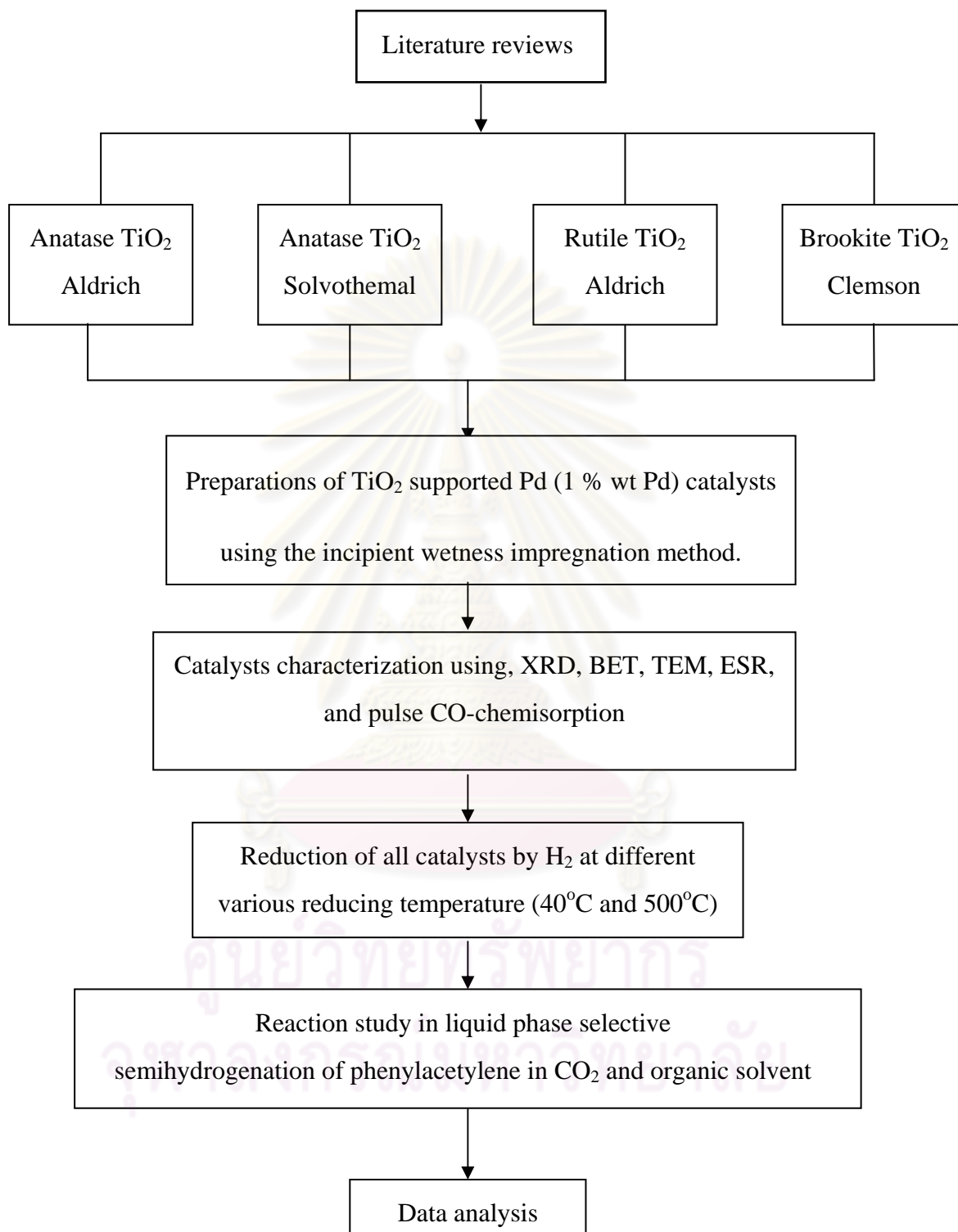


Figure 1.1 Flow diagram of research methodology

CHAPTER II

THEORY

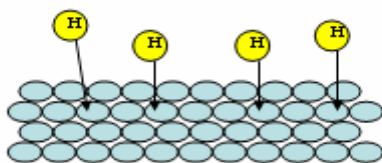
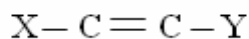
2.1 Selective Hydrogenation Reaction of Alkynes to Alkene

Hydrogenation is a class of chemical reactions which result in an addition of hydrogen (H₂) usually to unsaturated organic compounds. Typical substrates include alkenes, alkynes, ketones, nitriles, and imines. Most hydrogenations involve the direct addition of diatomic hydrogen (H₂) but some involve the alternative sources of hydrogen, not H₂: these processes are called transfer hydrogenations. The reverse reaction, removal of hydrogen, is called dehydrogenation.

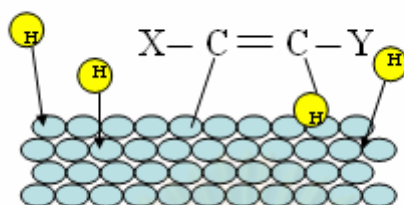
The classical example of a hydrogenation is the addition of hydrogen on unsaturated bonds between carbon atoms, converting alkenes to alkanes. Numerous important applications are found in the petrochemical, pharmaceutical and food industries. Health concerns associated with the hydrogenation of unsaturated fats to produce saturated fats and trans fats is an important aspect of current consumer awareness. Hydrogenation differs from protonation or hydride addition (e.g. use of sodium borohydride): in hydrogenation, the products have the same charge as the reactants

Selective hydrogenation reactions of alkynes to alkene are the reaction which take place on the surface of the metal catalyst. The mechanism of the reaction can be described in four steps :

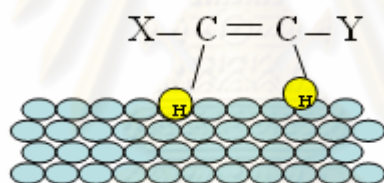
Step 1: Hydrogen molecules react with the metal atoms at the catalyst surface. The relatively strong H-H sigma bond is broken and replaced with two weak metal-H bonds.



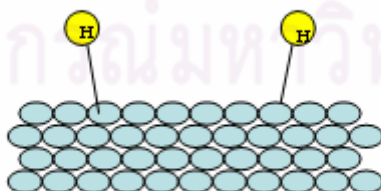
Step 2: The pi bond of the alkyne interacts with the metal catalyst weakening the bond. A hydrogen atom is transferred from the catalyst surface to one of the carbons of the triple bond.



Step 3: The pi bond of the alkyne interacts with the metal catalyst weakening the bond. A second hydrogen atom is transferred from the catalyst surface forming the alkene.



Step 4: The alkene is released from the catalyst's surface allowing the catalyst to accept additional hydrogen and alkene molecules.



Phenyl acetylene hydrogenation scheme consists of two consecutive steps in parallel with a single step directly to the final hydrogenation product.

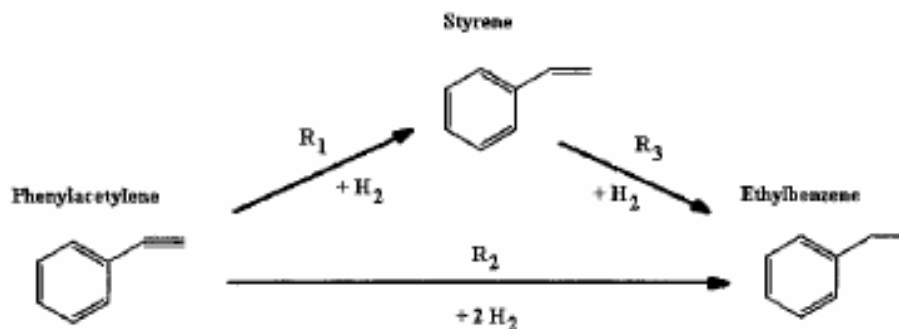


Figure 2.1 Scheme of Phenylacetylene hydrogenation (X. Huang *et al.*, 2003)

2.2 Physico-Chemical Properties of Supercritical Carbon Dioxide

The schematic representation of the phase diagram of pure carbon dioxide in Fig. 2.2 shows the aggregation state of CO₂ as a function of pressure and temperature. The solid, liquid, and gaseous state are separated by the melting, sublimation, and evaporation curve, respectively. These three states are in equilibrium at the triple point. The critical point marks the high-temperature end of the evaporation line and is characterized by the critical temperature $T_c=31.1$ °C and the critical pressure $p_c=73.8$ bar. No distinct liquid or vapor phase can exist beyond the critical point and the new supercritical phase has properties which are often reminiscent of both states. Similar to gases, scCO₂ has a very low surface tension, low viscosity, and high diffusion rates. Furthermore, scCO₂ forms fully homogeneous single phase mixtures with many reaction gases over a wide range of composition. On the other hand, the density of scCO₂ can easily be adjusted to liquid-like values and the solubility of liquid or solid material in these media can be orders of magnitude higher than predicted from the ideal gas law.

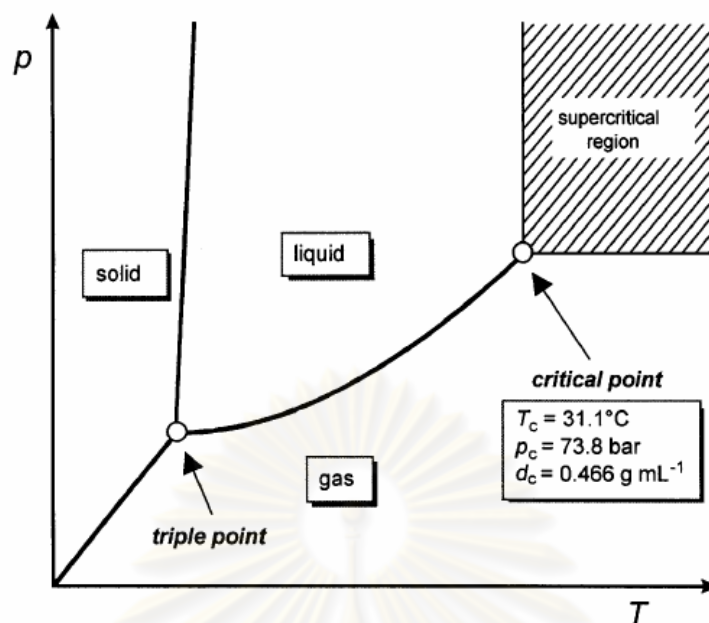


Figure 2.2 Schematic phase diagram of carbon dioxide (Walter Leitner)

The bulk density of CO_2 at the critical point ($d_c = 0.466 \text{ g mL}^{-1}$) is the mean value of the densities of the liquid and the gaseous phase just before entering the supercritical region. It must be noted, however, that the local density of an SCF is subject to large fluctuations and may differ considerably from the bulk density, especially around solute molecules. Many attempts have been made to utilize “chemical probes” like radical reactions or Diels-Alder additions to investigate these so-called clustering or augmentation phenomena. For most practical applications, however, it seems more important that the high compressibility of the supercritical phase allows the bulk density of scCO_2 to be varied continuously from very low to liquid-like values with relatively small variations in temperature and/or pressure. For example, the density of scCO_2 at 37°C is only 0.33 g mL^{-1} at 80 bar, but it rises to 0.80 g mL^{-1} at 150 bar.

2.3 Palladium

Palladium as a group VIII noble metal has unique catalytic properties in homogeneous and in heterogeneous reactions. In heterogeneous catalysis palladium is used for oxidation and hydrogenation reactions. One of the most remarkable properties of palladium is the ability to dissociate and dissolve hydrogen. Atomic hydrogen occupies the octahedral interstices between the Pd atoms of the cubic-closed packed metal. Palladium can absorb up to 935 times of its own volume of hydrogen. Depending on hydrogen partial pressure and temperature a so-called α - and β -hydride is formed.

Table 2.1 Physical properties of palladium.

atomic number	46
atomic weight	106.42 atomic
diameter	275.2 pm
melting point	1827 K
crystal structure	cubic closed packed
electron configuration	[Kr] 4d ¹⁰
electron negativity	1.4

Like other group VIII metals, palladium can be used for hydrogenation of unsaturated hydrocarbons. Palladium shows the highest selectivity of these metals in heterogeneously catalyzed semi-hydrogenation of alkynes and dienes to the corresponding alkenes (Amold *et al.*,1997). Activity of palladium for hydrocarbon hydrogenation is based on the ability for the dissociative adsorption of hydrogen and chemisorption of unsaturated hydrocarbons. The chemisorption of alkenes and alkynes is based on the interaction of the d-band of the Pd metal with the π -bonding system of the unsaturated hydrocarbons (Pallassana *et al.*,2000 and Mittendorfer *et al.*,2003). Industrially used catalysts for acetylene hydrogenation contain relatively

low Pd content (< 0.1 wt%) and are supported on metal oxides like alumina. Palladium shows high activity but only limited selectivity and long-term stability for hydrogenation of acetylene. The limited selectivity is mainly due to enhanced ethane formation and the formation of by-products like C_4 and higher hydrocarbons. Palladium shows a strong deactivation behavior because of hydrocarbon and carbon deposits. Catalyst deactivation by hydrocarbon and carbon deposits requires a frequent exchange or regeneration of the catalyst in the hydrogenation reactor. Moreover, fresh or regenerated catalysts show high activity and consequently lead to increased ethylene consumption and reduced selectivity. Furthermore, high activity of fresh or regenerated catalysts can lead to overheating (“thermal run away”) of the reactor because of the exothermic hydrogenation reaction.

2.4 Titanium (IV) oxide

Physical and chemical properties

Titanium (IV) oxide occurs naturally in three crystalline forms:

1. Rutile, which tends to be more stable at high temperatures. The application of almost rutile type is used in industrial products such as paints, cosmetics foodstuffs and sometimes found in igneous rocks.
2. Anatase, which tends to be more stable at lower temperatures. This type generally shows a higher photoactivity than other types of titanium dioxide.
3. Brookite, which is usually found only in minerals and has a structure belonging to orthorhombic crystal system.

A summary of the crystallographic properties of the three varieties is given in Table 2.2

Table 2.2 Crystallographic properties of anatase, brookite, and rutile.

Properties	Anatase	Brookite	Rutile
Crystal structure	Tetragonal	Orthorhombic	Tetragonal
Optical	Uniaxial, negative	Biaxial, positive	Uniaxial, negative
Density, g/cm ³	3.9	4.0	4.23
Hardness, Mohs scale	5 ^{1/2} – 6	5 ^{1/2} – 6	7 – 7 ^{1/2}
Unit cell	D _{4h} ¹⁹ .4TiO ₂	D _{2h} ¹⁵ .8TiO ₂	D _{4h} ¹² .3TiO ₂
Dimension, nm			
a	0.3758	0.9166	0.4584
b		0.5436	
c	0.9514	0.5135	2.953

Both of rutile and anatase type have a structure belonging to tetragonal crystal system but they are not isomorphous (Figure 2.2). The two tetragonal crystal types are more common because they are easy to make. Anatase occurs usually in near-regular octahedral, and rutile forms slender prismatic crystal, which are frequently twinned. Rutile is the thermally stable form and is one of the two most important ores of titanium.

The three allotropic forms of titanium dioxide have been prepared artificially but only rutile, the thermally stable form, has been obtained in the form of transparent large single crystal. The transformation from anatase to rutile is accompanied by the evolution of ca. 12.6 kJ/mol (3.01 kcal/mol), but the rate of transformation is greatly affected by temperature and by the presence of other substance which may either catalyze or inhibit the reaction. The lowest temperature at which conversion of anatase to rutile takes place at a measurable rate is ca. 700°C, but this is not a transition temperature. The change is not reversible; ΔG for the change from anatase to rutile is always negative.

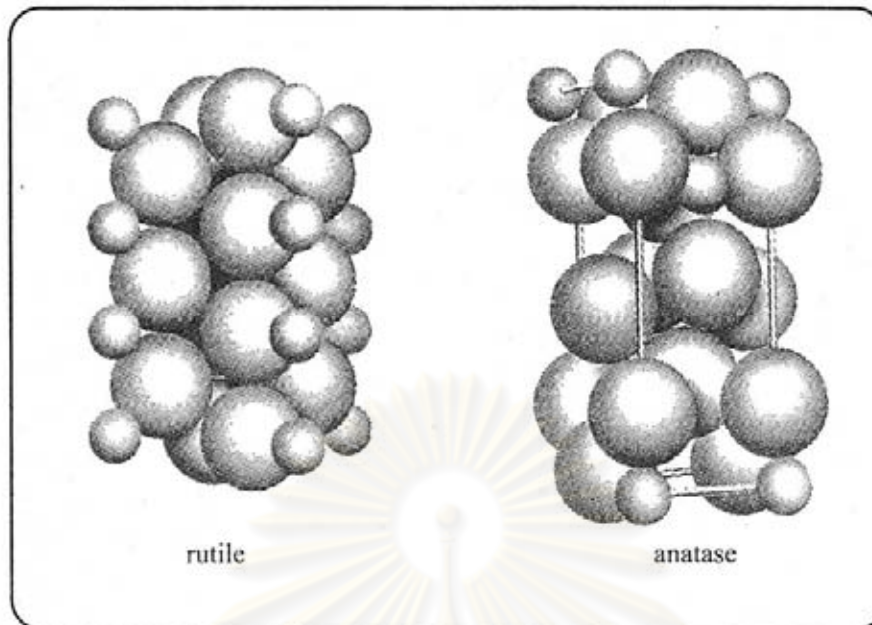


Figure 2.3 Crystal structure of TiO_2 . (Fujishima *et al.*, 1999)

Brookite has been produced by heating amorphous titanium (IV) oxide, prepared from an alkyl titanates of sodium titanate with sodium or potassium hydroxide in an autoclave at 200 to 600 °C for several days. The important commercial forms of titanium (IV) oxide are anatase and rutile, and these can readily be distinguished by X-ray diffraction spectrometry.

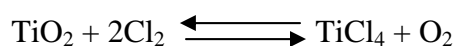
Since both anatase and rutile are tetragonal, they are both anisotropic, and their physical properties, e.g. refractive index, vary according to the direction relative to the crystal axes. In most applications of these substances, the distinction between crystallographic direction is lost because of the random orientation of large numbers of small particles, and it is mean value of the property that is significant.

Measurement of physical properties, in which the crystallographic directions are taken into account, may be made of both natural and synthetic rutile, natural anatase crystals, and natural brookite crystals. Measurements of the refractive index of titanium dioxide must be made by using a crystal that is suitably orientated with respect to the crystallographic axis as a prism in a spectrometer. Crystals of suitable size of all three modifications occur naturally and have been studied. However, rutile is the only form that can be obtained in large artificial crystals from melts. The

refractive index of rutile is 2.75. The dielectric constant of rutile varies with direction in the crystal and with any variation from the stoichiometric formula, TiO_2 ; an average value for rutile in powder form is 114. The dielectric constant of anatase powder is 48.

Titanium dioxide is thermally stable (mp 1855°C) and very resistant to chemical attack. When it is heated strongly under vacuum, there is a slight loss of oxygen corresponding to a change in composition to $\text{TiO}_{1.97}$. The product is dark blue but reverts to the original white color when it is heated in air.

Hydrogen and carbon monoxide reduce it only partially at high temperatures, yielding lower oxides or mixtures of carbide and lower oxides. At ca. 2000°C and under vacuum, carbon reduces it to titanium carbide. Reduction by metal, e.g., Na, K, Ca, and Mg, is not complete. Chlorination is only possible if a reducing agent is present; the position of equilibrium in the system is the reactivity of titanium dioxide towards acids is very dependent on the temperature to which it has been heated. For example, titanium dioxide that has been prepared by precipitation from a titanium (IV) solution and gently heated to remove water is soluble in concentrated hydrochloric acid. If the titanium dioxide is heated to ca. 900°C , then its solubility in acids is considerably reduced. It is slowly dissolved by hot concentrated sulfuric acid, the rate of solution being increased by the addition of ammonium sulfate, which raises the boiling point of the acid. The only other acid in which it is soluble is hydrofluoric acid, which is used extensively in the analysis of titanium dioxide for trace elements. Aqueous alkalis have virtually no effect, but molten sodium and potassium hydroxides, carbonates, and borates dissolve titanium dioxide readily. An equimolar molten mixture of sodium carbonate and sodium borate is particularly effective as is molten potassium pyrosulfate.



The reactivity of titanium dioxide towards acids is very dependent on the temperature to which it has been heated. For example, titanium dioxide that has been prepared by precipitation from a titanium (IV) solution and gently heated to remove

water is soluble in concentrated hydrochloric acid. If the titanium dioxide is heated to ca. 900°C, then its solubility in acids is considerably reduced. It is slowly dissolved by hot concentrate sulfuric acid, the rate of salvation being increased by the addition of ammonium sulfate, which raises the boiling point of the acid. The only other acid in which it is soluble is hydrofluoric acid, which is used extensively in the analysis of titanium dioxide for trace elements. Aqueous alkalies have virtually no effect, but molten sodium and potassium hydroxides, carbonates, and borates dissolve titanium dioxide readily. An equimolar molten mixture of sodium carbonate and sodium borate is particularly effective as is molten potassium pyrosulfate.



ศูนย์วิทยทรัพยากร
จุฬาลงกรณ์มหาวิทยาลัย

CHAPTER III

LITERATURE REVIEW

3.1 Synthesis of nanocrystalline TiO₂ by solvothermal method

M. Kang *et al.* (2001) synthesized TiO₂ photocatalysts by using the sol–gel and solvothermal methods in order to study renders a reliable synthesis procedure of the TiO₂ photocatalyst having the anatase structure of nano size. After that, physical properties and catalytic performances of two kinds TiO₂ photocatalysts were compared. The TiO₂ powder (Cat.2) obtained by the solvothermal method at 300°C exhibited a pure anatase structure without any further treatment, while the TiO₂ powder (Cat.1) prepared by the sol–gel method was transformed to the anatase structure after thermal treatment at 500°C for 3 h. Cat.2 had higher surface area (121m²/g) and surface charge (+24.1 mV) than Cat.1 (51m²/g, +16.4 mV).

C. K. Kim *et al.* (2003) synthesized TiO₂ nanoparticles in toluene solutions with titanium isopropoxide (TIP) by solvothermal methods. After synthesis at 250°C for 3 h with solutions at the weight ratios 10/100, 20/100 and 30/100 nanocrystalline TiO₂ particles are formed and they have a uniform anatase structure with average particle size below 20 nm. Average size of the nanocrystalline particle increases as increasing the amount of TIP precursor in this composition range. For the products obtained from the solution of 5/100 and 40/100, crystalline particles cannot be obtained. The 5/100 of TIP in the mixture may be too small amount to synthesize TiO₂ nanoparticles at 250°C and longer time is also needed to obtain adequate size of the particle. In the mixture of 40/100 TIP the synthetic process of TiO₂ particles may be hindered by agglomeration of the reactants due to surplus of precursor.

W. Kongsuebchart *et al.* (2006) synthesized nano-TiO₂ powder by solvothermal method under various reaction conditions in order to obtain average crystallite sizes of 9–15 nm. Increasing of titanium(IV)n-butoxide (TNB)

concentrations, the reaction temperatures, and the holding times resulted in an increase in the average crystallite size of TiO₂. The amounts of surface defect of TiO₂ were measured by means of temperature-programmed desorption of CO₂ and electron spin resonance spectroscopy. It was found that the ratios of surface defect/specific surface area increased significantly with increasing TiO₂ crystallite size. Moreover, the TiO₂ with higher amounts of surface defects exhibited much higher photocatalytic activity for ethylene decomposition.

3.2 Supported Pd catalyst in liquid-phase hydrogenation

J. Panpranot *et al.* (2006) studied liquid-phase hydrogenation of cyclohexene under mild conditions on Pd/SiO₂ in different organic solvents (benzene, heptanol, and NMP), under pressurized carbon dioxide, and under solvent less condition were investigated and compared. In the cases of using organic solvents, the hydrogenation rates depended on polarity of the solvents in which the reaction rates in high polar solvents such as heptanol and normal methyl pyrrolidone (NMP) were lower than that in a non-polar solvent. Hydrogenation rates were much higher when the reactions were performed under high-pressure CO₂ or under solvent less condition. The use of high-pressure CO₂ can probably enhance H₂ solubility in the substrate resulting in a higher hydrogenation activity. However, metal sintering and leaching in the presence of high-pressure CO₂ were comparable to those in organic solvents.

S. Domínguez-Domínguez *et al.* (2007) studied the differences supporting palladium colloids on three types of carbon supports: multiwall carbon nanotubes (NTs), carbon black (CB), and an activated carbon (AC). These catalysts were tested in a reaction of great industrial interest such as the partial hydrogenation of phenylacetylene. The liquid-phase hydrogenation reaction of phenylacetylene was performed under very mild conditions (323 K, flow of H₂ of 30 mL/min, 1 bar of pressure). The catalytic activities are very close to that of the homogeneous catalyst. A total conversion was achieved in all the Pd/C catalysts and also with very high selectivity toward styrene (higher than 95%). The carbon support produces

differences between the catalysts. The AC provokes a Pd particle agglomeration, and the catalyst has the lowest activity and selectivity. The highest selectivity is obtained for the Pd/NT sample. The ease of manipulation of the Pd/NT catalysts is noteworthy, facilitating its recovery by filtration and its subsequent reutilization. It was found that neither the catalytic activity nor the selectivity decreased appreciably throughout five consecutive cycles of the Pd/NT sample.

M. G. Musolino *et al.* (2007) studied the effect of metal particle size and supports of palladium catalysts in selective liquid phase conversion of cis-2-butene-1,4-diol affording also, when hydrogenated, 2-hydroxytetrahydrofuran.. Palladium catalysts on different supports (SiO_2 , Al_2O_3 , TiO_2 , ZrO_2 , MgO and ZnO) have been tested. The metal particle size was determined by TEM. The acidic properties of the catalysts were studied by FT-IR spectroscopy using pyridine as probe molecule. The influence of some preparative variables, such as the particle size, the support, the partial hydrogen pressure, on the catalytic behavior of palladium catalysts has been investigated. TEM measurements indicated that Pd particles diameter observed was in the range 2.5–10 nm. No significant variation of TOF and selectivity values with the metal particle size was observed in this range. Moreover, the activity and the selectivity towards reaction products were found to be strongly dependent on the acid–base characteristics of the support. The acid systems have been found more active and selective to isomerisation and hydrogenolysis products than the basic ones. No hydrogenolysis reaction was observed on basic supports. Among the examined catalysts, Pd/ TiO_2 resulted the most selective to 2-hydroxytetrahydrofuran. A maximum yield to this compound of about 74% was, in fact, obtained at 0.01 MPa of H_2 pressure.

3.3 Role of TiO_2 in selective hydrogenation

Y. Li *et al.* (2004) investigated in situ EPR and IR by using CO as probe molecules show that even pre-reduced by H_2 at lower temperature results in strong metal-support interaction (SMSI) for anatase titania supported palladium catalyst, but not for rutile titania supported palladium catalyst, which is attributed that the Ti^{3+} ions

produced by reduction of Ti^{4+} are fixed in the surface lattice of TiO_2 , as rutile titania is more thermodynamically and structurally stable than anatase titania so that the Ti^{3+} ions fixed in the surface lattice of anatase TiO_2 is easier to diffuse to surface of palladium particle than one in the surface lattice of rutile TiO_2 . The reason why the pre-reduction of both anatase and rutile supported palladium catalyst at higher temperature results in SMSI between Ti^{3+} and Pd is attributed that the thermal diffusion of produced Ti^{3+} ion at higher temperature is much easier than at lower temperature so that it could overcome the binding of surface lattice of both anatase and rutile titania to move to the surface or surrounding of palladium particle.

P. Weerachawanasak *et al.* (2007) investigate the SMSI phenomena and catalytic behavior of Pd catalysts supported on micron- and nano-size TiO_2 in liquid-phase selective hydrogenation of phenylacetylene under mild reaction conditions. It was found that when supported on the nano-sized TiO_2 , the Pd/ TiO_2 catalyst that reduced by H_2 at 500 °C exhibited strong metal–support interaction (SMSI) and much improved catalytic performance in liquid-phase selective hydrogenation of phenylacetylene. However, as revealed by CO pulse chemisorption, X-ray photoelectron spectroscopy (XPS), transmission electron microscopy (TEM), and CO-temperature program desorption, the SMSI effect was not detected for the micron-sized TiO_2 supported ones. It is suggested during high-temperature reduction, the inner Ti^{3+} in large crystallite size TiO_2 was more difficult to diffuse to the Pd^0 surface than the surface Ti^{3+} in the smaller crystallite size ones. Sintering of Pd^0 metal was observed instead.

3.4 Liquid phase hydrogenation in supercritical carbon dioxide

R. Tschan *et al.* (2001) studied continuous semihydrogenation of phenylacetylene over amorphous $\text{Pd}_{81}\text{Si}_{19}$ alloy in supercritical carbon dioxide. It was found that high conversion and selectivity were achieved over this catalyst without chemical modification, usually applied for Lindlar-type catalysts. Hydrogenation of PA to ST yielded the highest conversions and good selectivities at the edge of the sc

single-phase region. Moreover, excess hydrogen in the system leads to over hydrogenation of PA and thus to a steady decrease in selectivity.

M. Chatterjee *et al.* (2004) studied the differences supporting palladium such as MCM-48, SiO₂ and Al₂O₃ used in the selective hydrogenation of citral in scCO₂. The reported results show that it is possible to hydrogenate the conjugated and isolated C=C double bond forming a fully saturated aldehyde, dihydrocitronellal (3,7-dimethyloctanal) under mild conditions. The ascendancy of the scCO₂ medium is established in comparison with the conventional organic solvent and solventless conditions. Changes in different reaction parameters such as H₂ pressure, temperature and nature of the support do not affect the selectivity. Moreover, the catalyst can be recycled several times without any further treatment. Easy separation of the liquid product from the catalyst and the use of environmentally benign solvent make this procedure a viable and an attractive ideal green chemical process for large-scale application. Experimental findings are supported by the theoretical calculations to propose a plausible explanation for the reduction of the conjugated and isolated C=C double bonds in scCO₂.

R. Liu *et al.* (2007) studied the activity and selectivity of the transition metal complexes formed from Ru, Rh, Pd and Ni with triphenylphosphine (TPP) have been investigated for hydrogenation of citral in supercritical carbon dioxide (scCO₂). High activities are obtained with Ru/TPP and Pd/TPP catalysts, and the overall activity is in the order of Pd, Ru > Rh > Ni. The Ru/TPP complex is highly selective to the formation of unsaturated alcohols of geraniol and nerol. In contrast, the Pd/TPP catalyst is more selective to partially saturated aldehydes of citronellal. Furthermore, the influence of several parameters such as CO₂ and H₂ pressures, N₂ pressure and reaction time has been discussed. CO₂ pressure has a significant impact on the product distribution, and the selectivity for geraniol and nerol can be enhanced from 27% to 75% with increasing CO₂ pressure from 6 to 16 MPa, while the selectivity for citronellol decreases from 70% to 20%.

3.5 Comments on the previous works

From the previous studies, Pd is one of the most useful catalysts used in liquid-phase selective hydrogenation of alkyne to alkene. Furthermore, type of support shows the important roles in catalytic activity and selectivity. TiO₂ was selected as a candidate supports because it is well-known that it interacts strongly with Pd and it exhibits a strong metal-support interaction (SMSI). The SMSI phenomenon improved catalytic performance. The effect of TiO₂ polymorphs (anatase and rutile) on the strong metal-support interaction of Pd/TiO₂ has been studied and compared. It was shown that pre-reduction by H₂ at lower temperature results in SMSI for anatase titania supported palladium catalyst, but not for rutile titania supported one. Titania can be synthesized by various methods. Solvothermal method is an alternative route for one-step synthesis of pure anatase nano-sized TiO₂. In the recent years, supercritical carbon dioxide has been increasingly used as an environmentally friendly reaction medium in place of toxic and hazardous organic solvents. However, the effects of SMSI and supercritical carbon dioxide on Pd/TiO₂ have not been well studied so far. Thus, it is the aim of this study to investigate the catalytic behavior of TiO₂ supported palladium catalyst in the liquid phase selective hydrogenation under pressurized carbon dioxide and compare to that in organic solvent or the mixture of organic solvent and carbon dioxide.

CHAPTER IV

EXPERIMENTAL

This chapter describes the experimental procedure used in this research which can be divided into three sections. The catalyst preparation is shown in section 4.1. The reaction study in phenylacetylene hydrogenation is given in section 4.2. Finally, Properties of the catalyst characterized by various techniques are discussed in section 4.3

4.1 Catalyst Preparation

There are four types of TiO₂ supports used in this research. Anatase and Rutile TiO₂ was obtained commercially from Aldrich. Brookite TiO₂ prepared by school of Material science and Engineering, Clemson University and the nano-sized anatase TiO₂ used in this experimental were prepared by solvothermal method.

4.1.1 Preparation of TiO₂ supports using the solvothermal method

The chemicals used for TiO₂ supports preparation are shown in table 4.1.

Table 4.1 Chemicals used in the preparation of TiO₂

Chemical	Supplier
Titanium (IV) tert-butoxide (97% TNB, Ti[O(CH ₂) ₃ CH ₃] ₄)	Aldrich
1,4-butanediol (1,4-BG, HO(CH ₂) ₄ OH)	Aldrich
Methyl alcohol	Aldrich

The solvothermal-derived nano-TiO₂ supports were prepared by using specific amount of TNB as shown in Table 4.2. The starting material was suspended in 100 cm³ of 1, 4-butanediol in a test tube and put into the bigger test tube. The gap between the test tube and the autoclave wall was filled with 30 cm³ of the same solvent used in the test tube. Then setup both tubes into an autoclave. The autoclave was purged completely by nitrogen before heating temperature (see Table 4.2) at the rate of 2.5°C-min⁻¹. When the temperature was reached the autoclave was held at that temperature for specific time duration as shown in Table 4.2. The reaction performed inside autoclave during heat up and hold at constant temperature. When the desired holding time was achieved the reactor was cooled down to room temperature. The resulting powders were collected after repeated washing with methanol by centrifugation. They were then dried by air at room temperature. The schematic drawing of equipments used for TiO₂ support preparation are shown in Figure 4.1

Table 4.2 The condition used for the preparation of TiO₂

Conditions	Amount of TNB (g)	Solvent (1,4 Butanediol) (ml)	Temperature (°C)	Holding time (hr)
1	25	100	300	2

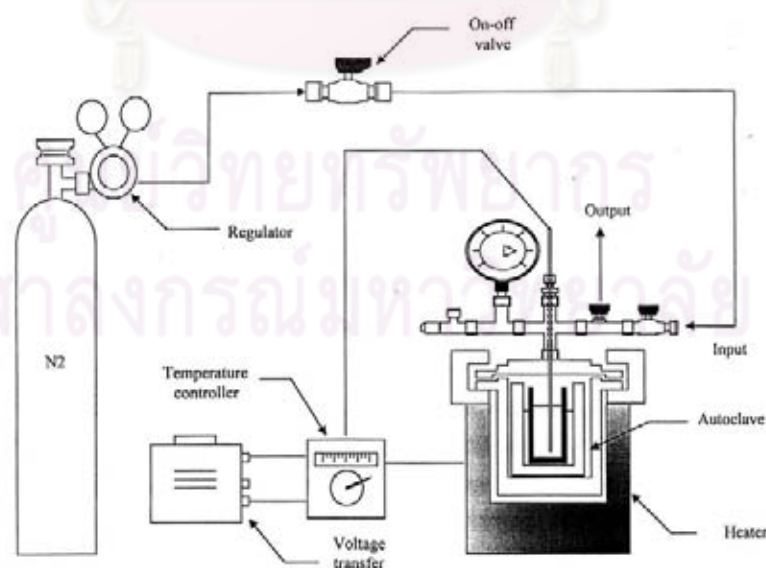


Figure 4.1 The schematic drawing of equipments used for the preparation of TiO₂.

4.1.2 Palladium Loading

In this experiment, incipient wetness impregnation is the method used for loading palladium. $\text{Pd}(\text{NO}_3)_2 \cdot 6\text{H}_2\text{O}$ is used as precursor in this methods. The incipient wetness impregnation procedure was as following:

1. The certain amount of palladium (1% loading) was introduced into the water which its volume equals to pore volume of catalyst.
2. TiO_2 support was impregnated with aqueous solution of palladium. The palladium solution is dropped slowly to the TiO_2 support.
3. The impregnated support was left to stand at room temperature for 6 hours to assure adequate distribution of metal complex. After that the catalyst was dried in the oven at 110°C overnight.
4. The catalyst is calcined in air at 450°C for 3 h.

4.2 The Reaction Study in Liquid-Phase Hydrogenation

The liquid-phase hydrogenation is used to study the characteristic and catalytic properties of these prepared catalysts. Phenylacetylene was used as reactants. Supercritical carbon dioxide and several organic solvents are used as reaction medium.

4.2.1 Chemicals and Reagents

The chemicals and reagents used in the reactions are shown in Table 4.3

Table 4.3 The chemicals and reagents used in the reaction

The chemicals and reagents	Supplier
High purity grade Hydrogen (99.99vol. %)	Thai Industrial Gases Limited
Carbon dioxide	Mallinckrodt
Absolute ethyl alcohol (99.99vol. %)	Aldrich
Phenylacetylene	Aldrich

4.2.2 Instruments and Apparatus

The schematic diagram of liquid-phase hydrogenation is shown in Figure 4.2. The main instruments and apparatus are explained as follow:

The autoclave reactor

The 50 ml stainless steel autoclave was used as reactor. Hot plate stirrer with magnetic bar was used to heat up the reactant and to ensure that the reactant and the catalyst are well mixed.

Supercritical carbon dioxide pump

The PU-1580-CO₂ is a liquid CO₂ delivery system using SSQD (Slow Suction Quick Delivery) method. The maximum usable pressure is 30 MPa. The operating temperature range is between 10 to 30°C.

GC-MS

Table 4.4 Operating conditions for GC-MS

Inlets	Gas He (99.99%) Heater 250°C Pressure 3.14 psi Total Flow 14.1 ml/min
Columns	Mode Constant Flow Installed Column HP-5MS, 0.25mm*30m*0.25um Pressure 3.14 psi Flow 0.5 ml/min Average Velocity 26 cm/sec
Oven	Set point 100°C
Aux	Set point 250°C
MS	Aaq Mode scan
Edit Scan Params	Start-end 50-750

4.2.3 Liquid-Phase Hydrogenation Procedure

The liquid-phase hydrogenation of phenylacetylene was carried out in two steps. The first step was catalyst preparation and the second step was hydrogenation study.

1. Reduction step

Approximately 0.2 gram of supported Pd catalyst was placed into the U-tube of Micromeritic. After that, the catalyst was reduced by the hydrogen gas at the volumetric flow rate of 50 ml/min at 40°C and 500°C for 2 h.

2. Reactant preparation and hydrogenation step

The hydrogenation of phenylacetylene was carried out in a stainless steel batch reactor (50 ml). Certain amounts of catalyst (0.005 gram) and the reactant (1 ml of phenylacetylene and 9 ml of ethanol) were loaded into the reactor and then the reactor was sealed and flushed with 1 MPa H₂ twice. After the reactor was heated up to a reaction temperature of 313 K, first H₂ and then CO₂ were introduced into the reactor to a certain pressure using a high-pressure liquid pump. The reaction mixture was stirred continuously with a magnetic bar during the reaction. Then the reactor was cooled to room temperature and depressurized carefully by a backpressure regulator. The product mixture was analyzed by gas chromatography with flame ionization detector (FID) and the catalyst was characterized by several techniques.

ศูนย์วิทยทรัพยากร
จุฬาลงกรณ์มหาวิทยาลัย

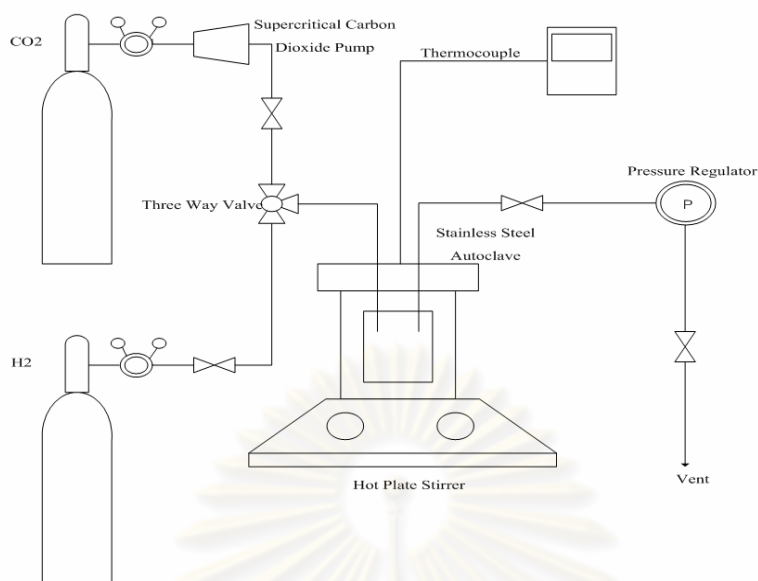


Figure 4.2 The schematic diagram of liquid-phase hydrogenation

4.3 Catalyst Characterization

The fresh and spent catalysts were characterized by several techniques such as

4.3.1 X-ray Diffraction (XRD)

The bulk crystal structure and chemical phase composition were determined by diffraction of an X-ray beam as a function of the angle of the incident beam. The XRD spectrum of the catalyst was measured by using a SIEMENS D5000 X-ray diffractometer and $\text{CuK}\alpha$ radiation with Ni filter in the 2θ range of 20-80 degrees resolution 0.04° . The crystallite size was calculated from Scherrer's equation.

4.3.2 N_2 Physisorption

The BET surface area of sample, average pore size diameters and pore size distribution were determined by physisorption of nitrogen (N_2) using Micromeritics ASAP 2020 (surface area and porosity analyzer). Each sample was degassed under

vacuum pressure $<10 \mu\text{m Hg}$ in the Micromeritics system at 150°C for 4 h prior to N_2 physisorption.

4.3.3 Transmission Electron Microscopy (TEM)

The palladium oxide particle size and distribution of palladium on titanium supported catalysts were observed using AJEM-200CX transmission electron microscope operated at 160 kV at the Scientific and Technological Research Equipment Center (STREC), Chulalongkorn University.

4.3.4 Scanning Electron Microscopy (SEM)

Catalysts granule morphology and elemental distribution were obtained using a JEOL JSM-35F scanning electron microscope. The SEM was operated using the back scattering electron (BSE) mode at 20 kV at the Scientific and Technological Research Equipment Center, Chulalongkorn University (STREC)

4.3.5 CO-Pulse Chemisorption

The active sites and the relative percentages dispersion of palladium catalyst were determined by CO-pulse chemisorption technique using Micromeritics ChemiSorb 2750 (pulse chemisorption system). The known amount of CO was pulsed into the catalyst bed at room temperature. Carbon monoxide that was not adsorbed was measured using thermal conductivity detector. Pulsing was continued until catalyst surface was saturated with CO. The number of metal active sites was calculated in the basic assumption that only one CO molecule adsorbed on one metal active site (Anderson *et al.*, 1995, Ali *et al.*, 1998 and Mahata *et al.*, 2000).

Approximately 0.2 g of catalyst was filled in a u-tube, incorporated in a temperature-controlled oven and connected to a thermal conductivity detector (TCD). He was introduced into the reactor at the flow rate of 30 ml/min in order to remove remaining air. Prior to chemisorption, the samples were reduced in a H_2 flow rate at 50 ml/min with heated at an increasing rate of $10^\circ\text{C}/\text{min}$ from room temperature to 40°C or 500°C and held at this temperature for 2 h. After that cooled down to ambient

temperature in a He flow, then CO was plus into the catalyst bed at room temperature. Carbon monoxide that was not adsorbed was measured using thermal conductivity detector. Pulsing was continued until no further carbon monoxide adsorption was observed. Calculation details of %metal dispersion are given in Appendix C.

4.3.6 Electron Spin Resonance (ESR)

ESR will be performed to determine the defect of surface catalysts by JEOL JAPAN. The ESR using model JES-RE2X at the Scientific and Technological Research Equipment Center, Chulalongkorn University (STREC)



CHAPTER V

RESULTS AND DISCUSSION

This thesis was conducted in order to investigate the characteristics and catalytic properties of TiO₂-An, TiO₂-Ru, TiO₂-Br and TiO₂-SV supported Pd catalysts in liquid phase semihydrogenation of phenylacetylene to styrene in scCO₂. In this chapter, the experimental results and discussions are described. The results and discussions are divided into two main sections. The first part describes the characteristics of TiO₂ supports and Pd/TiO₂ catalysts (section 5.1). The catalysts were characterized by several techniques such as XRD, N₂ physisorption, SEM, TEM, ESR and CO-pulse chemisorption. The second part, liquid-phase semihydrogenation of phenylacetylene in scCO₂ has been investigated on a several TiO₂ supported Pd catalysts (section 5.2).

5.1 Characterization of TiO₂ supports and Pd/TiO₂ catalysts

5.1.1 X-Ray Diffraction (XRD)

Bulk crystal structure and chemical phase composition of a crystalline material having crystal domains of greater than 3-5 nm can be detected by diffraction of an X-ray beam as a function of the angle of the incident beam. The measurements were carried out at the diffraction angles (2θ) between 20° and 80°. Broadening of the diffraction peaks were used to estimate crystallite diameter from Scherrer Equation. The phase composition of titania was calculated from the following equation used by Zhang and Banfield:

$$W_A = \frac{k_A A_A}{k_A A_A + A_R + k_B A_B}$$

$$W_B = \frac{k_B A_B}{k_A A_A + A_R + k_B A_B}$$

$$W_R = \frac{k_R A_R}{k_A A_A + A_R + k_B A_B}$$

where W_A , W_B and W_R represent the weight fractions of the anatase, brookite, and rutile phases, respectively; k_A is 0.886 and k_B is 2.721; A_A , A_B and A_R are the integrated intensities of the anatase ($2\theta=25^\circ$), brookite ($2\theta=31^\circ$) and rutile ($2\theta=28^\circ$) peaks, respectively (Zhang and Banfield, 2000).

The XRD patterns of TiO_2 samples are shown in Figure 5.1. TiO_2 -An and TiO_2 -SV exhibited the characteristic peaks of the anatase TiO_2 at 25° (major), 37° , 48° , 55° , 56° , 62° , 71° , and 75° . TiO_2 -Ru exhibited the characteristic peaks of the rutile TiO_2 at 28° (major), 36° , 42° , and 57° . XRD peaks at 26° and 31° (major) for TiO_2 -Br were evident. The average crystallite sizes and percent of TiO_2 phase composition contained in each sample are shown in Table 5.1. The average crystallite size of TiO_2 -An, TiO_2 -SV and TiO_2 -Br calculated from the full width at half maximum of the XRD peak using Scherrer equation were 90 nm, 12 nm and 6.4 nm, respectively. For TiO_2 -Ru could not be determined by this method due to the calculation limit of the Scherrer equation (the crystallite size may be too large). The phase composition of TiO_2 -An and TiO_2 -SV showed almost pure anatase titania (~ 97-98%). TiO_2 -Ru showed 93% rutile titania and TiO_2 -Br was mixed phases of 53% brookite, 45% anatase, and 2% rutile.

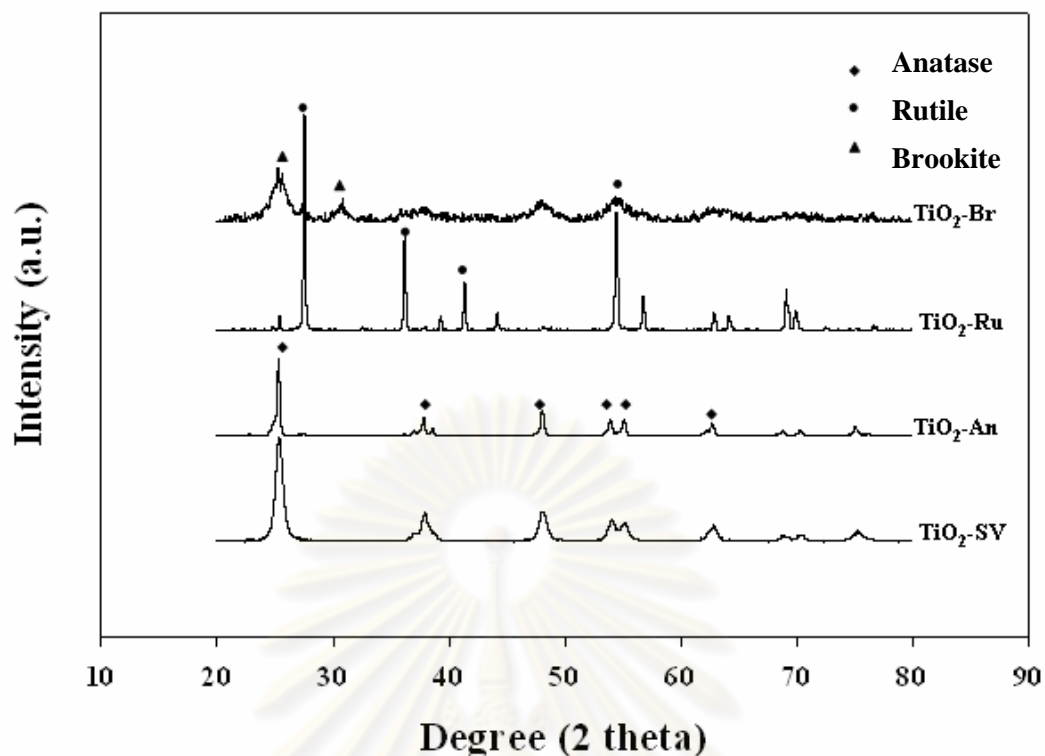


Figure 5.1 The XRD patterns of the TiO₂ polymorphs. An, Anatases; Ru, Rutile; Br, Brookite; SV, Solvolthermal

The XRD patterns of the titania after impregnation with palladium, calcinations, and reduction at 40°C (R40) and 500°C (R500) are shown in Figure 5.2 and Figure 5.3. The XRD characteristic peaks corresponding to PdO ($2\theta = 33.9^\circ$) and Pd⁰ ($2\theta = 40.2^\circ$ and 46.7°) were not detected in all cases due probably to the low amount of palladium present or it was in a highly dispersed form.

The average crystallite sizes of 1%Pd/TiO₂ catalysts were calculated from the Scherrer equation (see in Table 5.1). When 1%Pd/TiO₂-An was reduced at 40°C and 500°C, the crystallite sizes of TiO₂ were 100 and 134 nm, respectively. The crystallite sizes of 1%Pd/TiO₂-Br increased from 8.7 to 13.4 nm when reduced at 40°C and 500°C, respectively. While 1%Pd/TiO₂-SV after reduction at 40°C and 500°C, the crystallite sizes of TiO₂ were 12.5 and 13.4 nm, respectively. It was found that the reduction with H₂ either 40°C or 500°C did not result in significant changes of the TiO₂ crystallite sizes. However, a slight increase in TiO₂ crystallite sizes were probably caused by high temperature calcinations and reduction of catalysts at 500°C.

Similar results were also observed by Patcharaporn Weerachawansak et al. (Patcharaporn Weerachawansak *et al.*, 2008) for crystallite sizes of the TiO₂-nano. Besides, there is no phase change for all titania supports when reduced at 500°C except for titania Brookite. After reduced at high temperature, predominant phase 53% brookite changed to 78% rutile (see in **Table 5.1**). This result was also observed by Christopher et al. (Christopher *et al.* 2007)

Table 5.1 The crystallite sizes and phase composition of TiO₂ support and 1%Pd/TiO₂ catalysts

Sample	%Content of TiO ₂ phase (wt.%)			Crystallite sizes of TiO ₂ (nm)
	An	Ru	Br	
TiO ₂ -An	97.0	0.9	2.1	90.0
1%Pd/TiO ₂ -An R40	97.0	0.9	2.1	100.0
1%Pd/TiO ₂ -An R500	97.0	0.9	2.1	134.0
TiO ₂ -Ru	4.7	93.0	2.3	n.d.
1%Pd/TiO ₂ -Ru R40	4.7	93.0	2.3	n.d.
1%Pd/TiO ₂ -Ru R500	4.7	93.0	2.3	n.d.
TiO ₂ -Br	45.0	2.0	53.0	6.4
1%Pd/TiO ₂ -Br R40	45.0	2.0	53.0	8.7
1%Pd/TiO ₂ -Br R500	3.0	78.0	17.0	13.4
TiO ₂ -SV	98.0	0.0	2.0	12.0
1%Pd/TiO ₂ -SV R40	98.0	0.0	2.0	12.5
1%Pd/TiO ₂ -SV R500	98.0	0.0	2.0	13.4

n.d. = not determined.

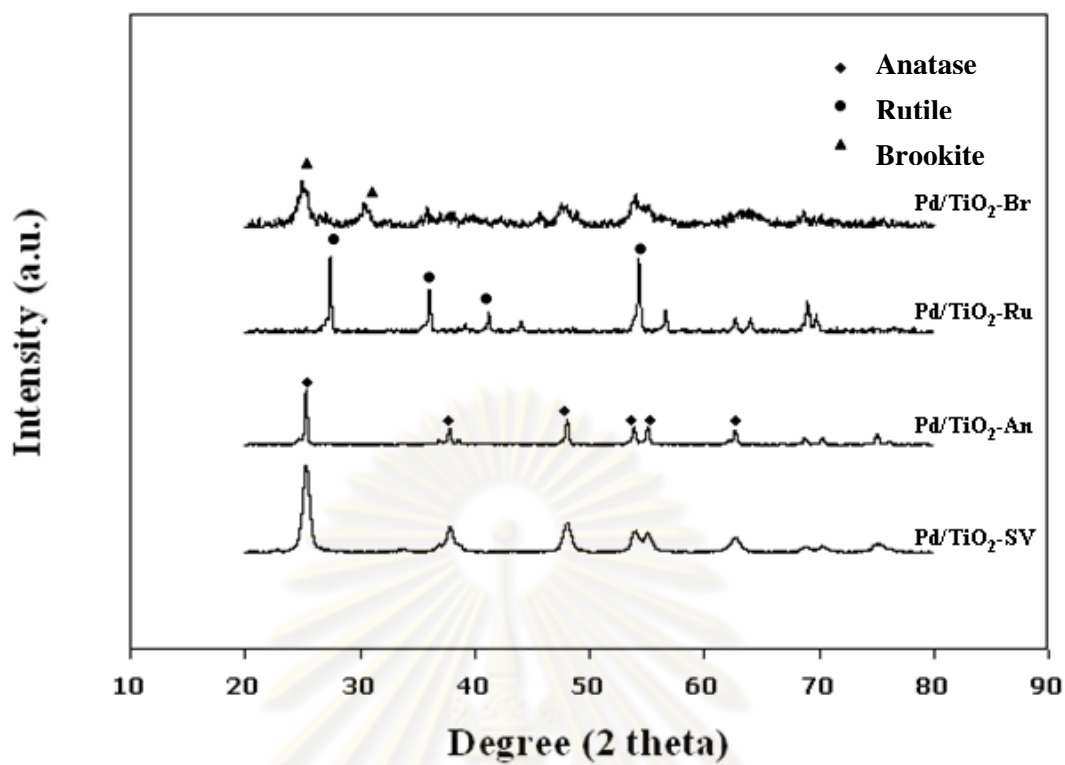


Figure 5.2 The XRD patterns of 1%Pd/TiO₂ when reduced at 40°C

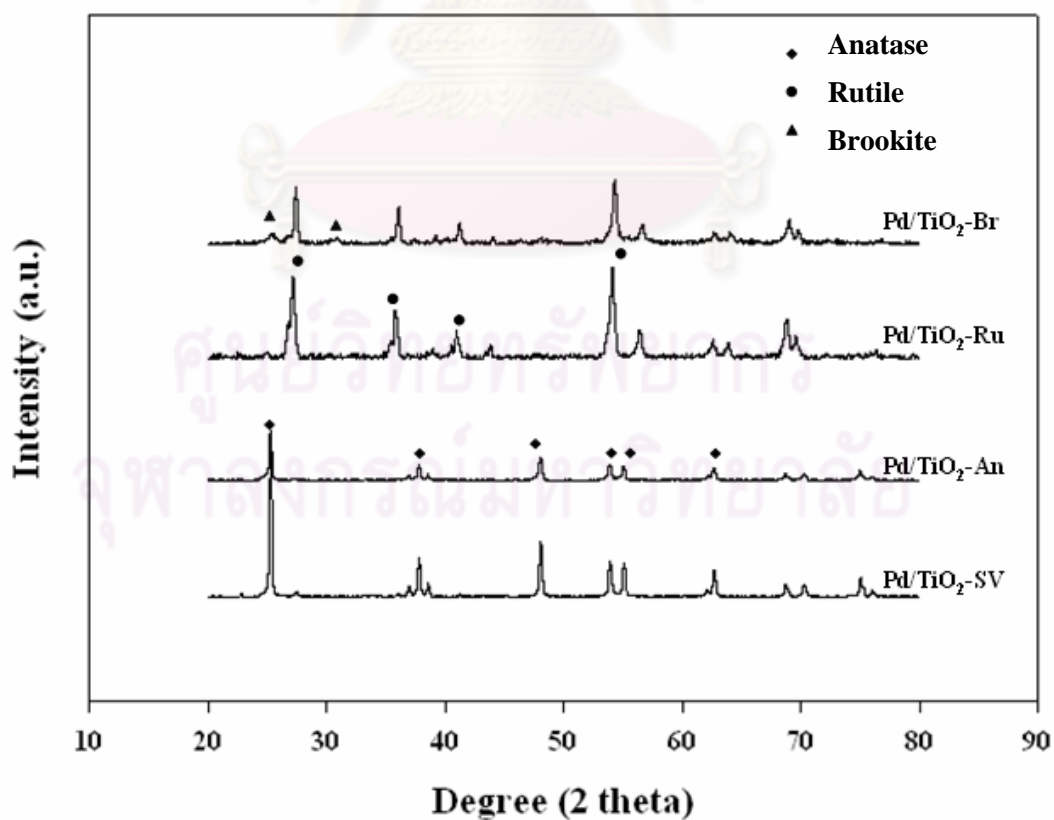


Figure 5.3 The XRD patterns of 1%Pd/TiO₂ when reduced at 500°C

5.1.2 N₂ Physisorption

The results of BET surface area, pore volume and average pore diameter analysis of TiO₂ and the Pd supported on TiO₂ catalysts which determined by N₂ physisorption technique are given in Table 5.2. The BET surface area of TiO₂-Ru, TiO₂-An, TiO₂-SV and TiO₂-Br were 2.2, 9.0, 85.0 and 147.6 m²/g, respectively. The BET surface area of TiO₂-SV and TiO₂-Br were found to be higher than that of TiO₂-An and TiO₂-Ru because both titania supports were nanocrystalline. Thus BET surface area were much higher than TiO₂-An and TiO₂-Ru. Moreover, it was indicated by Brunauer-Emmet-Teller (BET) method that the pores of all TiO₂ supports were mesopore. The pore volumes TiO₂-Ru, TiO₂-An, TiO₂-Br and TiO₂-SV were 0.003, 0.021, 0.09 and 0.3 cm³/g, respectively.

The BET surface area of 1%Pd/TiO₂-An and 1%Pd/TiO₂-Ru reduced at 40°C were 10.5 and 2.3 m²/g, respectively. Then after reduction at 500°C the BET surface area was 9.7 and 2.2 m²/g, respectively. It can be seen that BET surface areas of the catalysts slightly decreased. There were no significantly differences between the BET surface area of the 1%Pd/TiO₂ and the original TiO₂ support suggesting that most of the palladium were deposited on the external surface of the support. In contrast, the BET surface areas of 1%Pd/TiO₂-Br and 1%Pd/TiO₂-SV catalysts rapidly decreased after reduction at 500°C. Such results indicate that pore blockage or destruction of the TiO₂ pore structure occurred for these cases. These results corresponded to the decrease of TiO₂-Br pore volume for 1%Pd/TiO₂-Br-R40 and 1%Pd/TiO₂-Br-R500 from 0.09 to 0.09 and 0.06 cm³/g, respectively. The pore volumes TiO₂-SV, 1%Pd/TiO₂-SV-R40 and 1%Pd/TiO₂-SV-R500 were 0.3, 0.3, and 0.2 cm³/g, respectively.

Table 5.2 N₂ physisorption properties of TiO₂ supports and Pd supported on TiO₂ catalysts

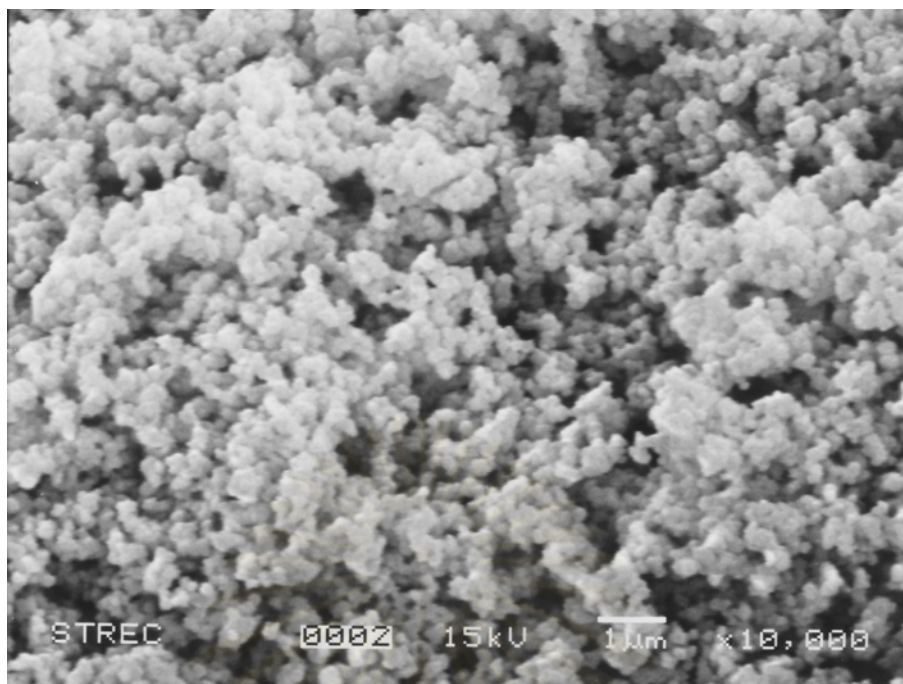
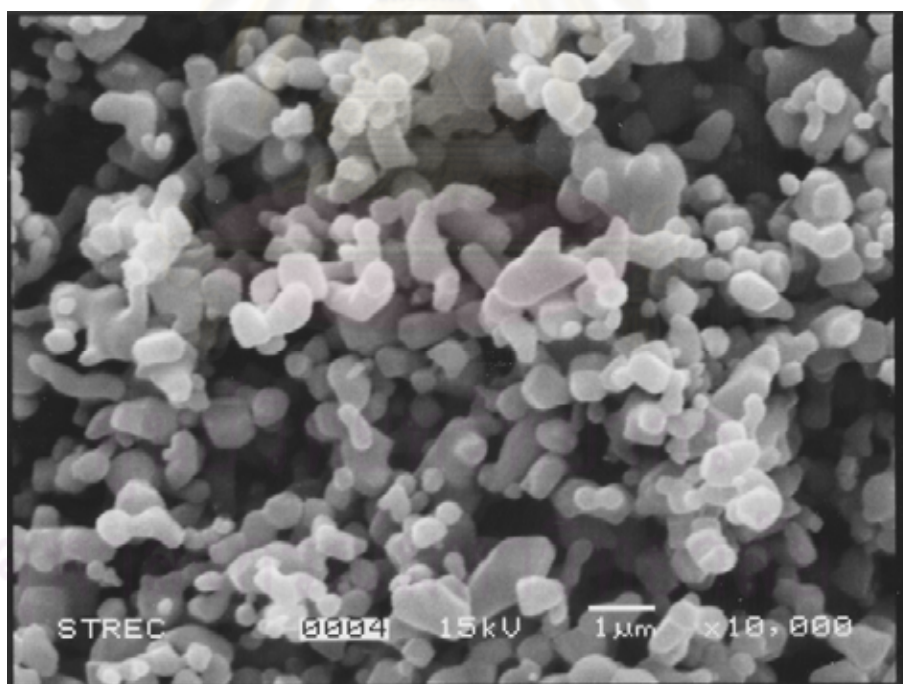
Samples	BET surface area (m²/g)	Pore volume (cm³/g)	Pore diameter (nm)
TiO ₂ -An	9.0	0.021	9.7
TiO ₂ -Ru	2.2	0.003	44.5
TiO ₂ -Br	147.6	0.090	2.4
TiO ₂ -SV	85.0	0.300	12.0
1%Pd/TiO ₂ -An-R40	10.5	0.03	13.3
1%Pd/TiO ₂ -An-R500	9.7	0.03	12.1
1%Pd/TiO ₂ -Ru-R40	2.3	0.005	33.5
1%Pd/TiO ₂ -Ru-R500	2.2	0.003	43.1
1%Pd/TiO ₂ -Br-R40	68.5	0.09	3.3
1%Pd/TiO ₂ -Br-R500	23.4	0.06	6.6
1%Pd/TiO ₂ -SV-R40	101	0.3	7.9
1%Pd/TiO ₂ -SV-R500	78	0.2	7.7

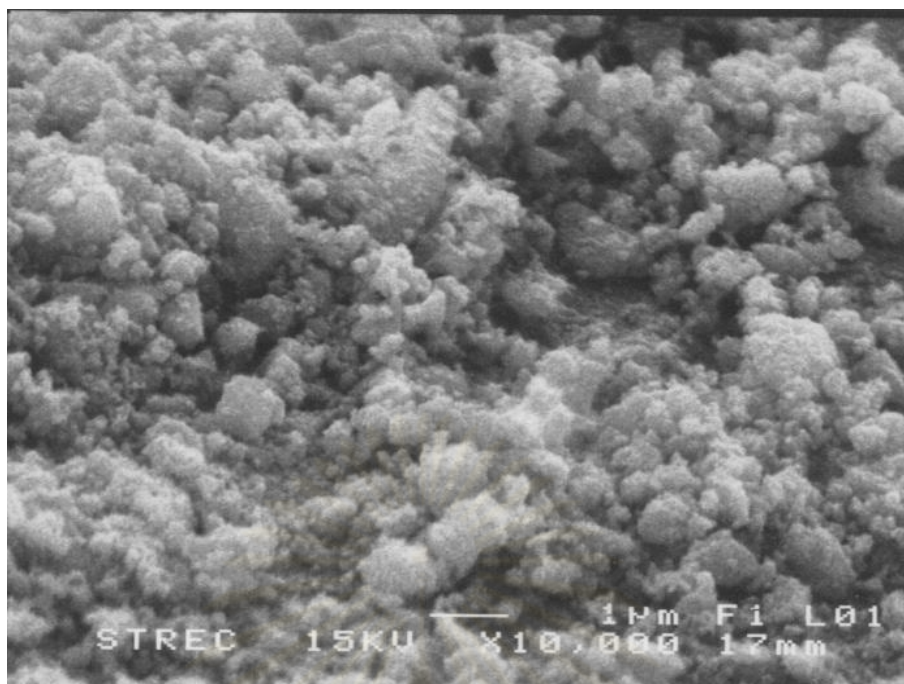
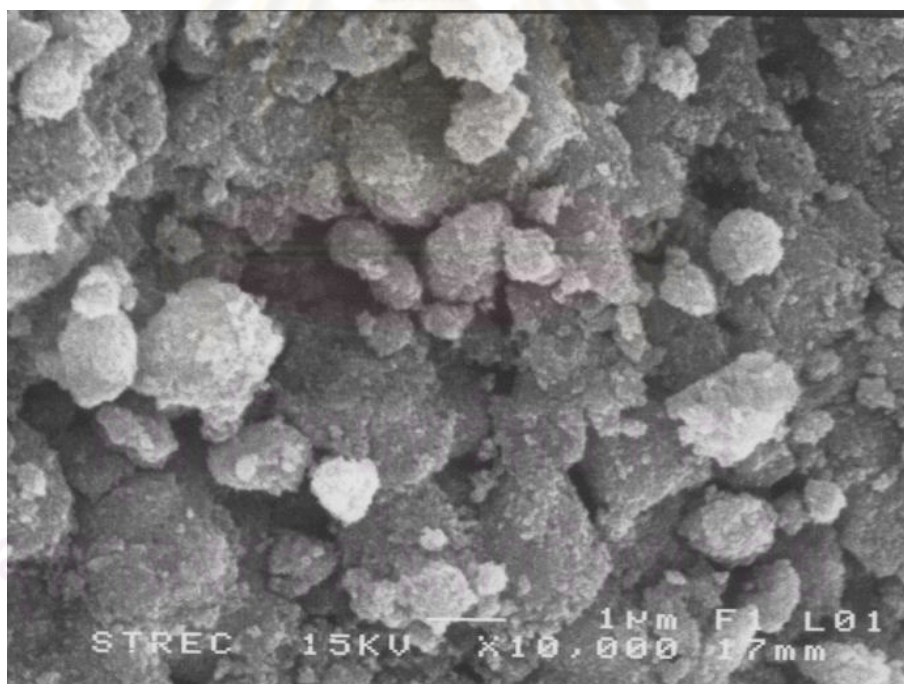
ศูนย์วิทยทรัพยากร
จุฬาลงกรณ์มหาวิทยาลัย

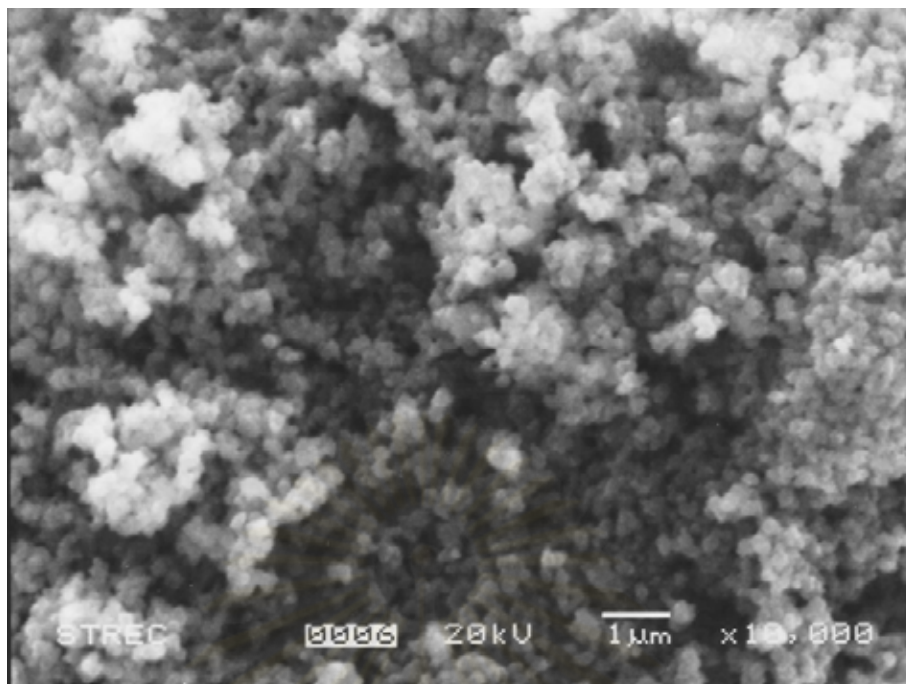
5.1.3 Scanning Electron Microscopy (SEM)

Scanning electron microscopy (SEM) is a powerful tool for direct observing surface texture and morphology of catalyst materials. In the backscattering scanning mode, the electron beam focused on the sample is scanned by a set of deflection coils. Backscattered electrons or secondary electrons emitted from the sample are detected.

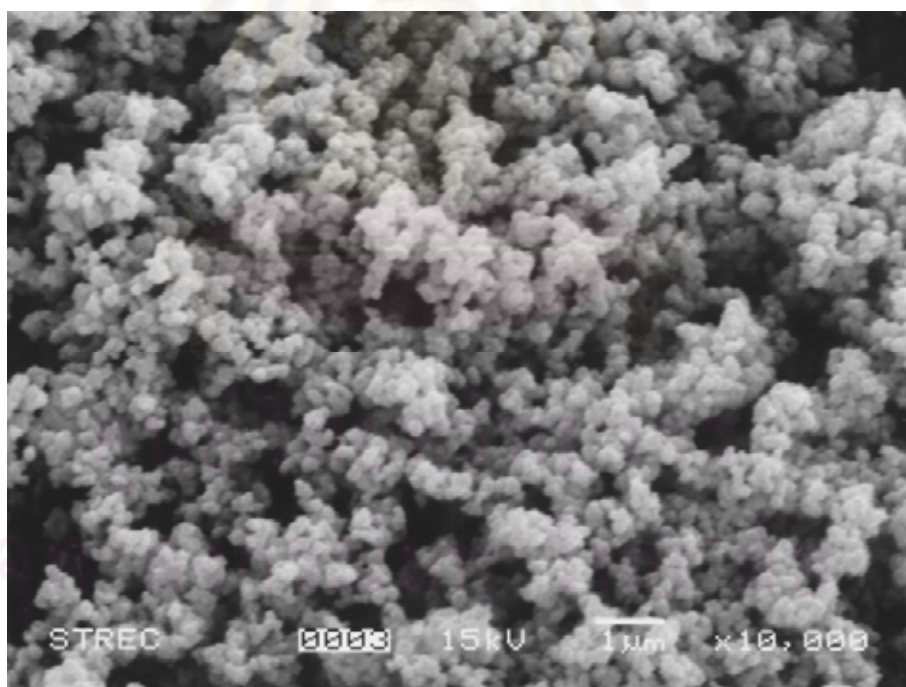
The SEM micrograph of different TiO₂ supports and 1 wt% Pd/TiO₂ catalysts after reduced at 40 and 500°C are shown in Figure 5.4. As it can be seen, particles had a fairly monodisperse size distribution for all of the samples. The morphologies of TiO₂-Br and TiO₂-SV consisted of irregular shape of very fine particles agglomerated while particles of TiO₂-An and TiO₂-Ru were uniform and round shape. Besides, morphologies of the reduced 1%Pd/TiO₂ catalysts were not significantly different from TiO₂ supports. The primary particle of TiO₂ supports were not found and the crystallite sizes of all TiO₂ samples can be not determined because the SEM technique had resolution in micron scale. However, the crystallite sizes of all TiO₂ samples were confirmed by TEM technique.

(A) TiO₂-An(B) TiO₂-Ru

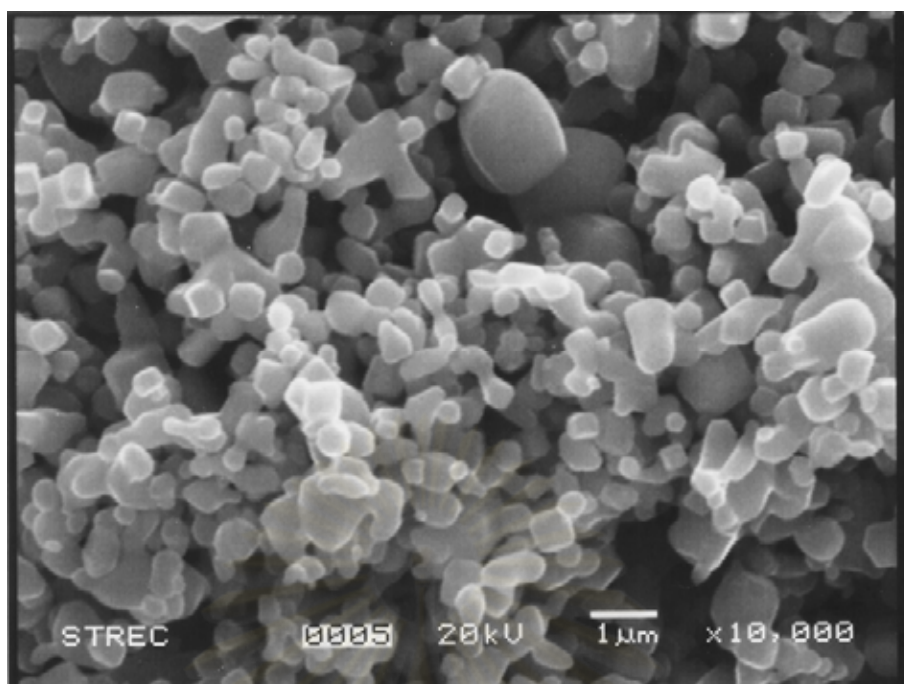
(C) TiO₂-Br(D) TiO₂-SV



(E) 1%Pd/TiO₂-An-R40



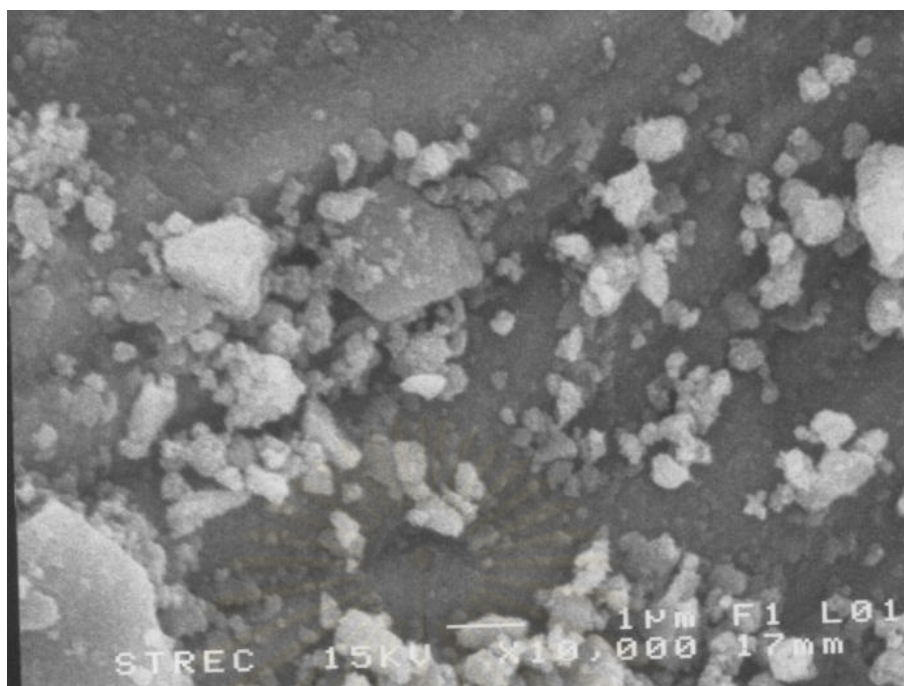
(E) 1%Pd/TiO₂-An-R500



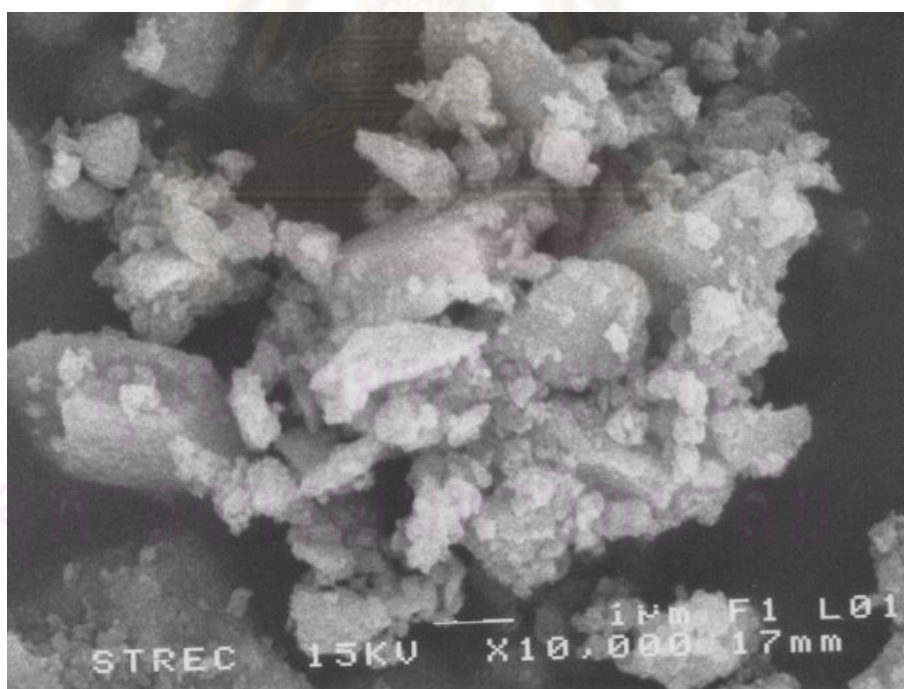
(G) 1%Pd/TiO₂-Ru-R40



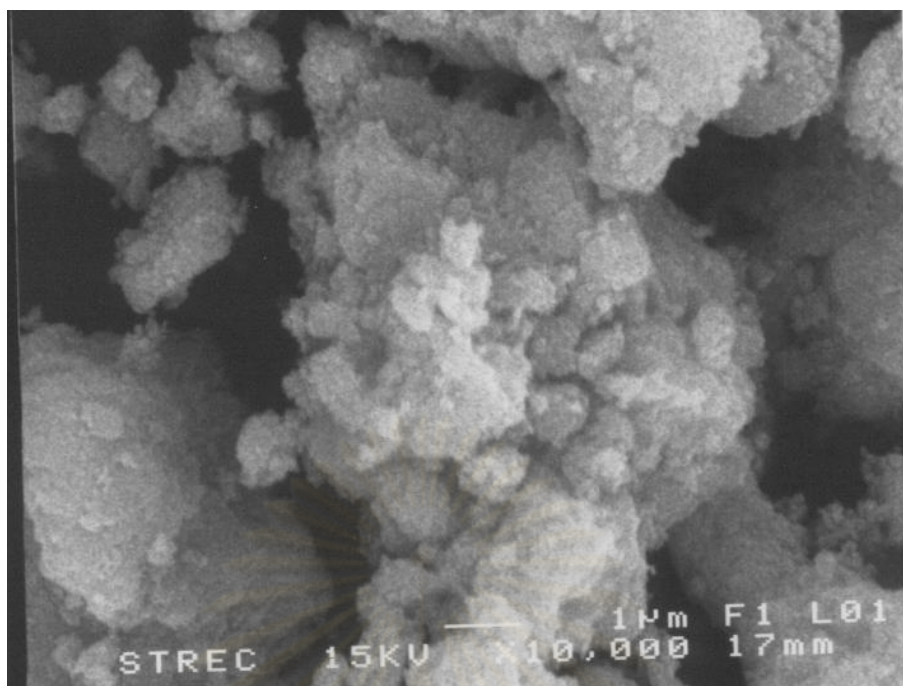
(H) 1%Pd/TiO₂-Ru-R500



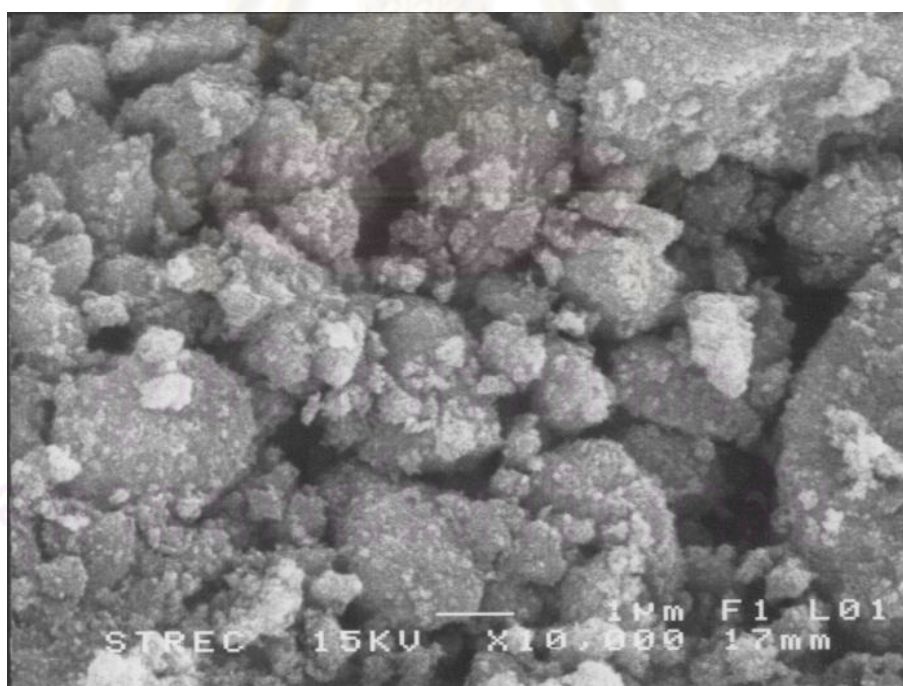
(I) 1%Pd/TiO₂-Br-R40



(J) 1%Pd/TiO₂-Br-R500



(K) 1%Pd/TiO₂-SV-R40



(L) 1%Pd/TiO₂-SV-R500

Figure 5.4 SEM micrographs of TiO₂ supports and Pd supported on TiO₂ catalysts

5.1.4 Transmission Electron Microscopy (TEM)

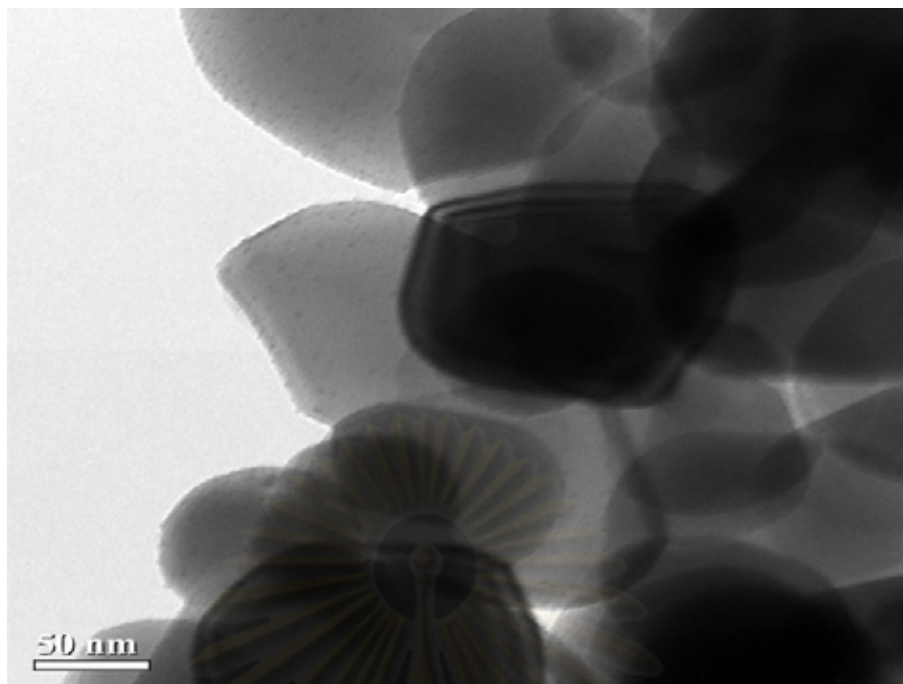
TEM is a useful tool for determining crystallite size and size distribution of supported metals. It allows determination of the micro-texture and microstructure of electron transparent samples by transmission of a focused parallel electron beam to a fluorescent screen with a resolution presently better than 0.2 nm.

TEM analysis has been carried out in order to physically measure the TiO₂ crystallite size and the Pd⁰ particle sizes on the various 1%Pd/TiO₂ catalysts. Table 5.3 exhibited the crystallite size of different TiO₂ supports that calculated from XRD and TEM. It was observed that the crystallite size of different TiO₂ supports increased in the order TiO₂-Br > TiO₂-SV > TiO₂-An > TiO₂-Ru. Reduction with H₂ either at 40 and 500°C did not result in significant changes of the TiO₂ crystallite sizes. TEM results were shown in Figure 5.5. It was seen that on the TiO₂-An, Pd⁰ metal particle sizes increased when the catalysts were reduced at 500°C. Such results indicated that sintering of Pd⁰ metal occurred on the 1%Pd/TiO₂ catalyst during high temperature reduction. Moreover, for the Pd/TiO₂-Ru, Pd/TiO₂-Br and Pd/TiO₂-SV after reduced at 40 and 500°C, the presence of Pd particles were not clearly seen as on the Pd/TiO₂-An.

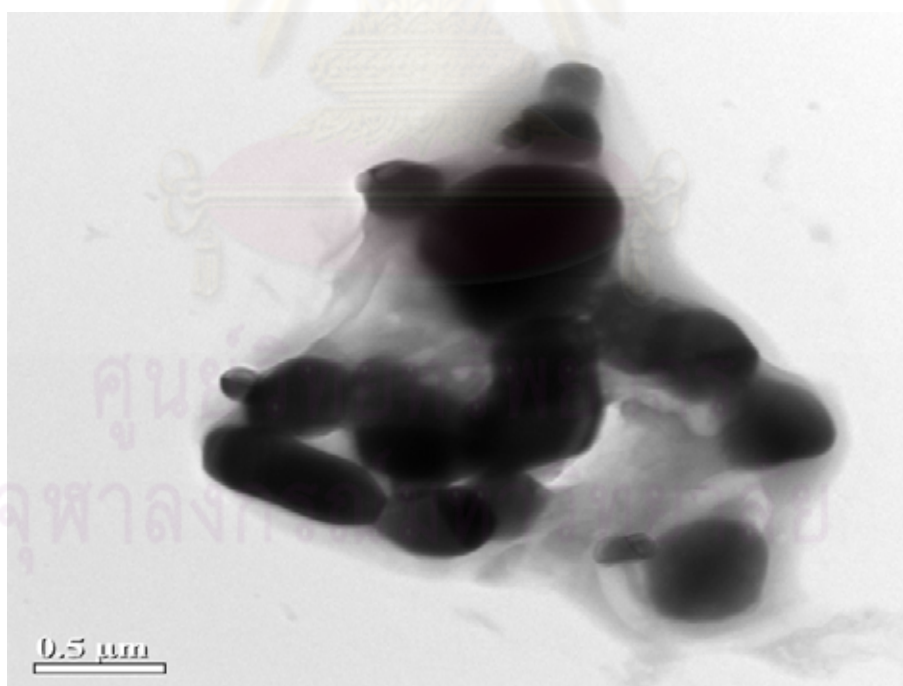
Table 5.3 The crystallite sizes of difference TiO₂ support

Sample	Crystallite sizes of TiO ₂ from XRD (nm)	Crystallite sizes of TiO ₂ from TEM (nm)
TiO ₂ -An	90.0	100
TiO ₂ -Ru	n.d.	400
TiO ₂ -Br	6.4	7
TiO ₂ -SV	12.0	13

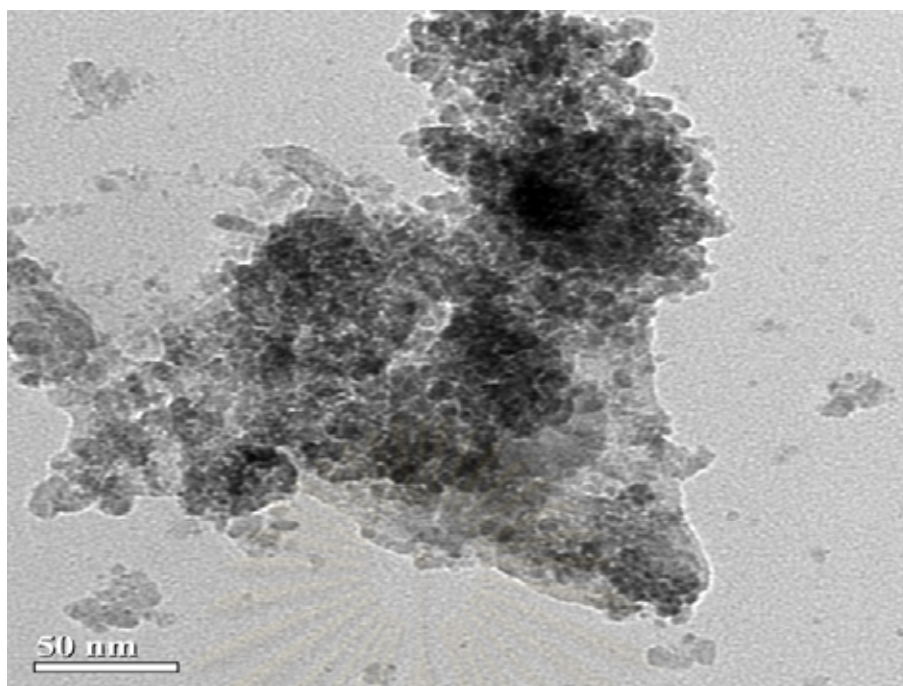
n.d. = not determined.



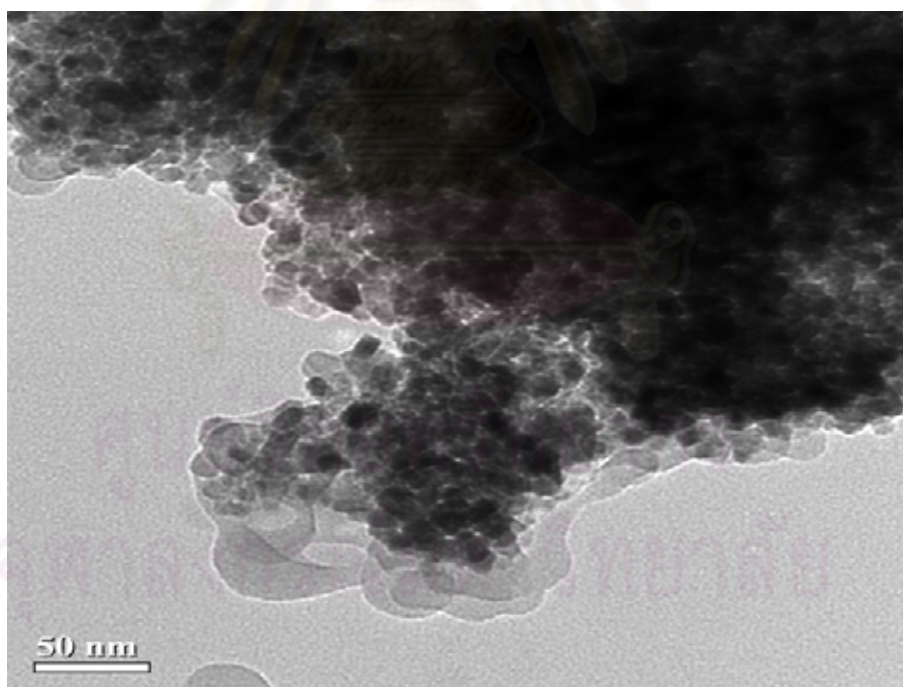
(A) $\text{TiO}_2\text{-An}$



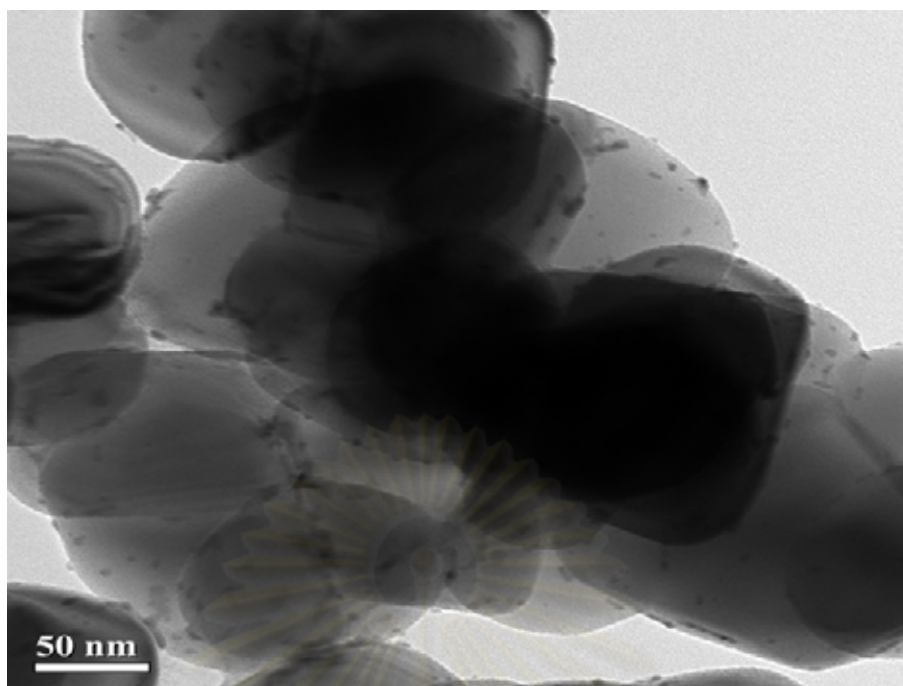
(B) $\text{TiO}_2\text{-Ru}$



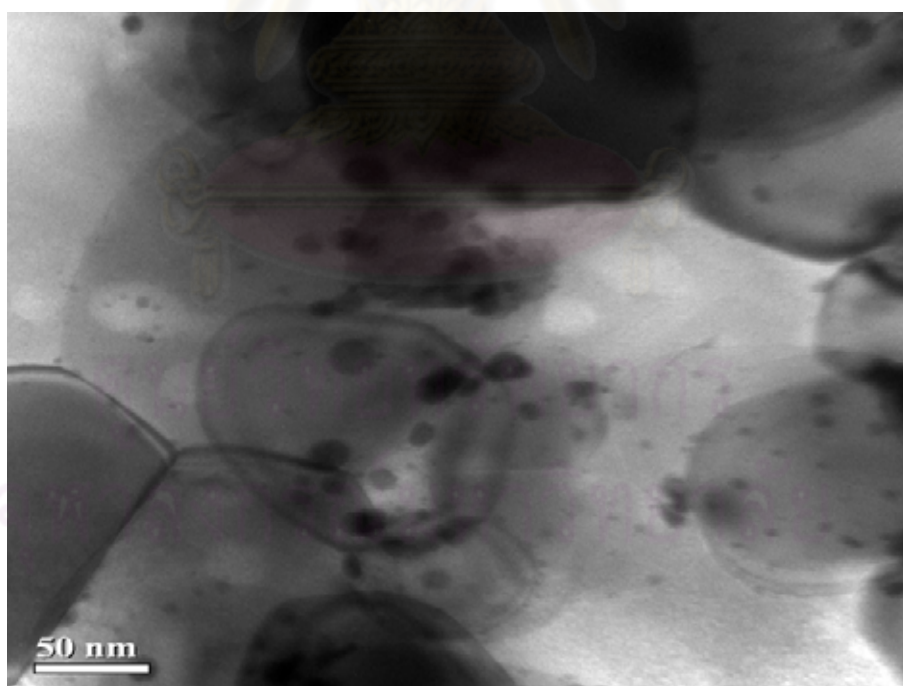
(C) $\text{TiO}_2\text{-Br}$



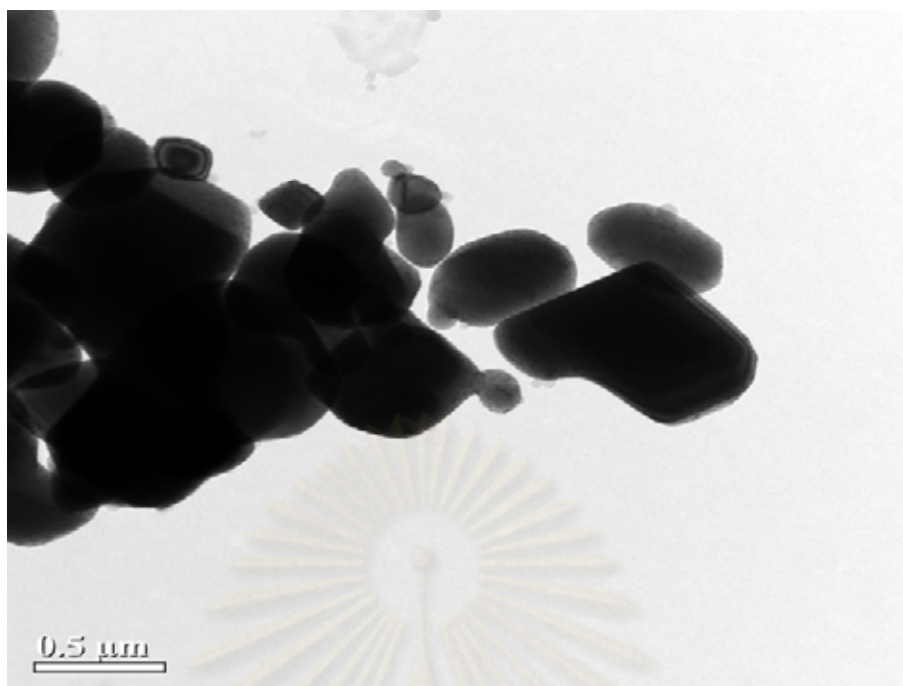
(D) $\text{TiO}_2\text{-SV}$



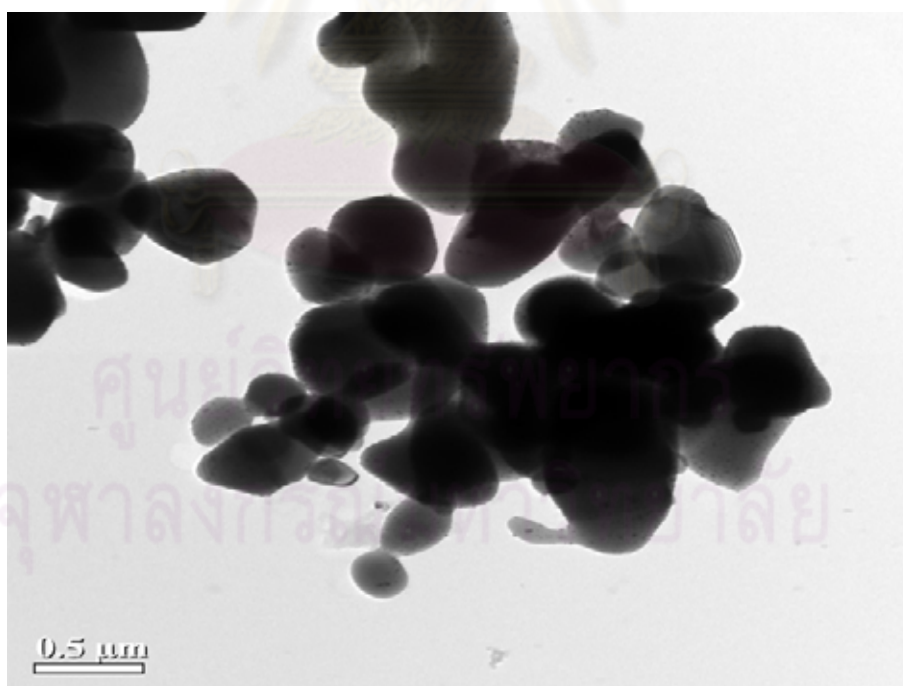
(E) 1%Pd/TiO₂-An R40



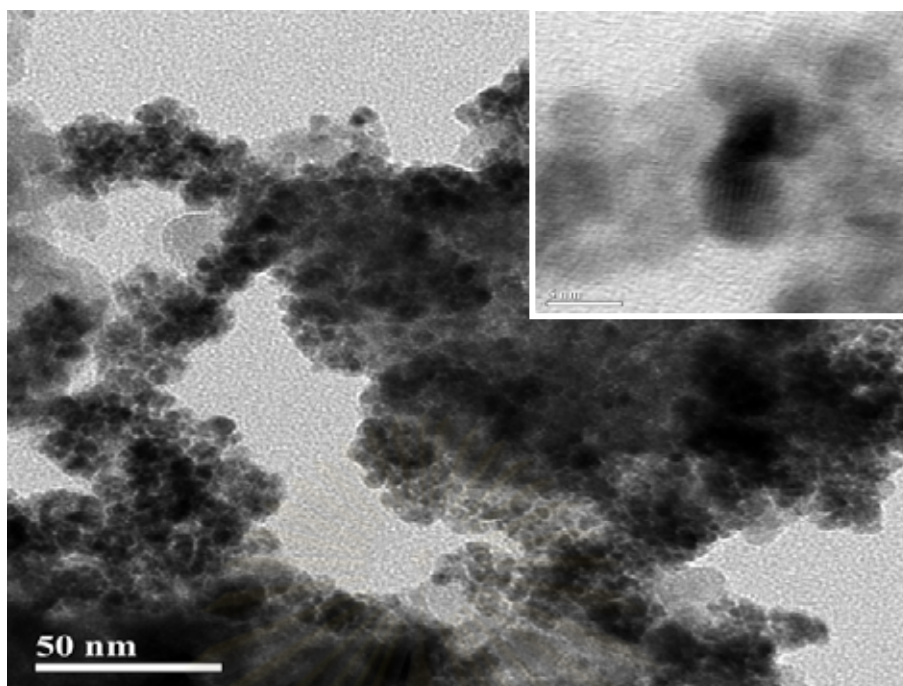
(F) 1%Pd/TiO₂-An-R500



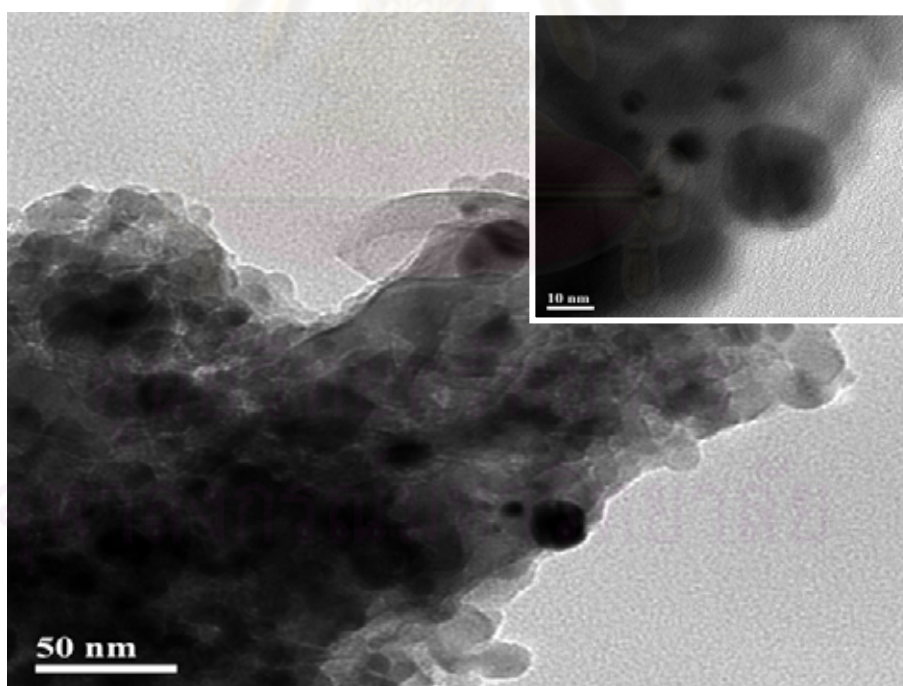
(G) 1%Pd/TiO₂-Ru-R40



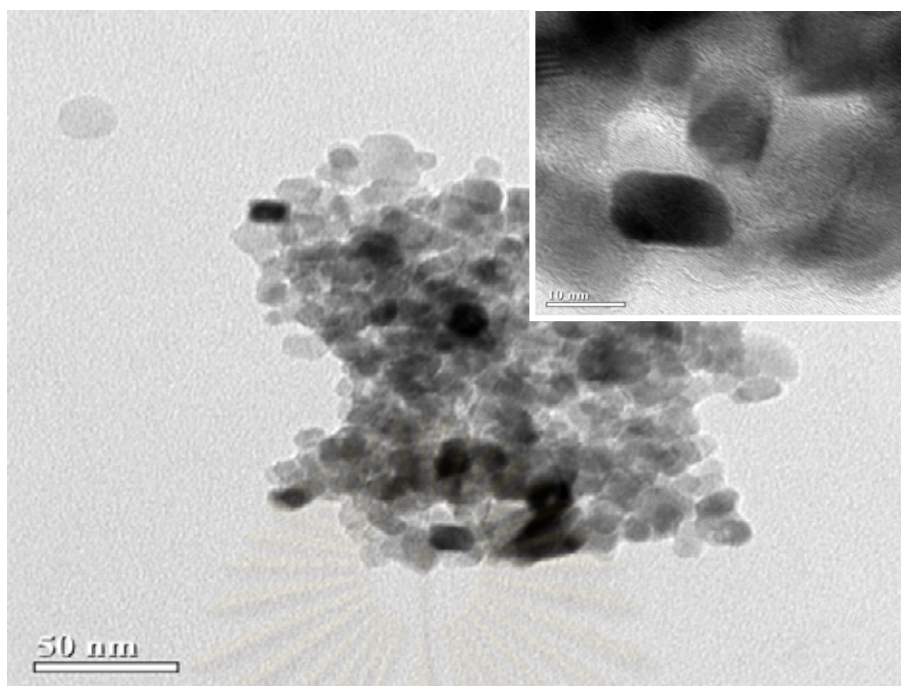
(H) 1%Pd/TiO₂-Ru-R500



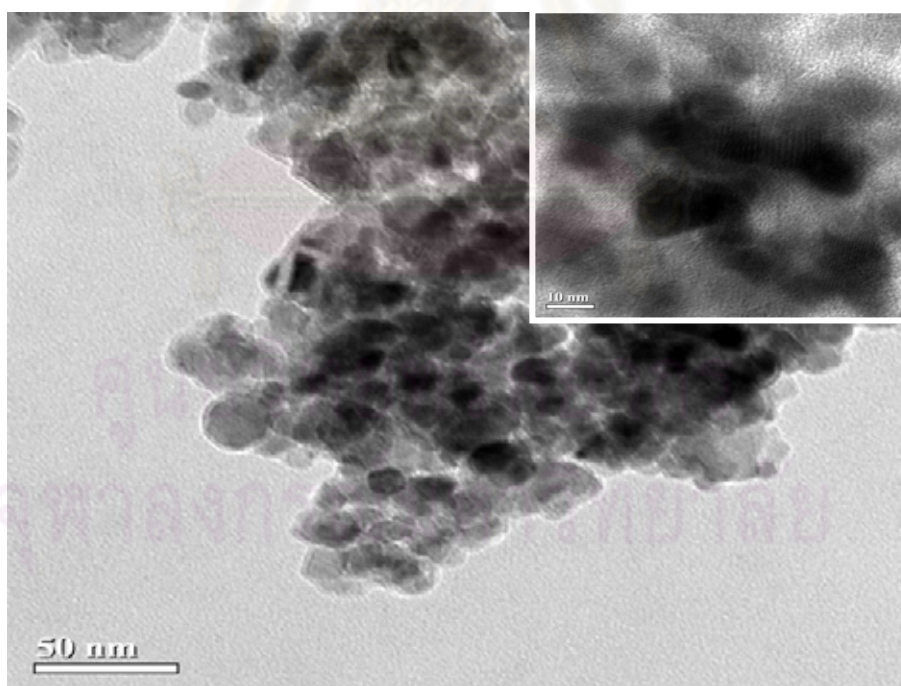
(I) 1%Pd/TiO₂-Br-R40



(J) 1%Pd/TiO₂-Br-R500



(K) 1%Pd/TiO₂-SV-R40



(L) 1%Pd/TiO₂-SV-R500

Figure 5.5 TEM micrographs of TiO₂ supports and Pd supported on TiO₂ catalysts

5.1.5 Metal active sites

The metal active sites measurement is based on chemisorption technique. Chemisorption is relatively strong, selective adsorption of chemically reactive gases available on the metal sites or the metal oxide surfaces at relatively higher temperatures (i.e. 25-400°C); the adsorbate-adsorbent interaction involves with formation of chemical bonds and heats of chemisorption in the order of 50-300 kJ mol⁻¹. The active surface areas of Pd of the catalysts were calculated from the irreversible pulse CO chemisorption technique based on the assumption that one CO molecule adsorbs on one palladium site (Anderson *et al.*, 1985, Ali and Goodwin, 1998, Sales *et al.*, 1999 and Mahata *et al.*, 2000). The total CO chemisorption, palladium particle sites and palladium dispersion of catalysts when reduced at 40°C and 500°C are reported in Table 5.3.

The amount of CO chemisorption of catalysts reduced at 40°C were 15.3x10¹⁸, 10.8x10¹⁸, 10.6x10¹⁸ and 8.5x10¹⁸ molecule CO/g.cat for 1%Pd/TiO₂-SV, 1%Pd/TiO₂-Br, 1%Pd/TiO₂-An and 1%Pd/TiO₂-Ru, respectively. This was probably due to the lower percentage of Pd dispersion. For all the catalysts, the amount of CO chemisorption was much lower when reduced at 500°C. The amount of CO chemisorption were 1.8x10¹⁸, 1.6x10¹⁸, 1.5x10¹⁸ and 1.2x10¹⁸ molecule CO/g.cat for 1%Pd/TiO₂-SV, 1%Pd/TiO₂-Ru, 1%Pd/TiO₂-An and 1%Pd/TiO₂-Br, respectively. From XRD results of catalysts reduced at 500°C (see Figure 5.3), it is noticed that the brookite TiO₂ transformed to rutile phase TiO₂ upon reduction at 500°C, re-calcination, and re-reduced at 40°C. The amount of CO chemisorption on 1%Pd/TiO₂-Br was lower than 1%Pd/TiO₂-Ru. Thus, the presence of rutile phase significantly lower amount of CO chemisorption. The Pd⁰ metal particle sizes calculated from CO chemisorption of the catalysts reduced at 40°C were found to be 4.2–6.7 nm. The results were consistent with TEM analysis. For the catalysts reduced at 500°C, the Pd⁰ metal particle sizes of 1%Pd/TiO₂-An and Ru were increased to 38.2 and 32.7 nm. For 1%Pd/TiO₂-Br and 1%Pd/TiO₂-SV, the Pd⁰ metal particle sizes were not determined due to poor contrast in THE images.

Table 5.4 Results from CO chemisorption of Pd supported on TiO₂ catalysts

Catalysts	CO chemisorption (*10 ¹⁸ site/g.cat)	%Pd dispersion	d _p Pd ⁰ (nm)
1%Pd/TiO ₂ -An R40	10.6	19.0	5.9
1%Pd/TiO ₂ -An R500	1.5	2.9	38.2
1%Pd/TiO ₂ -Ru R40	8.5	16.7	6.7
1%Pd/TiO ₂ -Ru R500	1.6	3.4	32.7
1%Pd/TiO ₂ -Br R40	10.8	21.3	5.3
1%Pd/TiO ₂ -Br R500	1.2	n.d.	n.d.
1%Pd/TiO ₂ -SV R40	15.3	26.5	4.2
1%Pd/TiO ₂ -SV R500	1.8	n.d.	n.d.

n.d. = not determined

5.1.6 Strong Metal Support Interaction Test (SMSI Test)

The SMSI effect was probably similar to the decoration of metal surface by partially reducing metal oxides after high temperature reduction on these catalysts (Tauster *et al.*, 1978). It was confirmed by measuring the amounts of CO chemisorption of the re-calcined (at 450°C) and re-reduced (at 40°C) catalysts after they were subjected to reduction at 500°C. If the catalyst has the SMSI effect, the metal active site can be totally recovered after SMSI test. Because of notable feature of SMSI, it is reversed by oxidizing conditions.

The results are illustrated in Figure 5.6. It was found that the amount of CO chemisorption of the re-calcined and re-reduced 1%Pd/TiO₂-An and 1%Pd/TiO₂-Ru were less than that reduced at 40°C suggesting that sintering of the palladium particles occurred during high temperature reduction as indicated by larger Pd particle size from TEM. On the other hand, the amount of CO chemisorption of the re-calcined and re-reduced 1%Pd/TiO₂-Br and 1%Pd/TiO₂-SV could be totally recovered

indicating that the palladium particles did not sinter and exhibited the SMSI effect. Recent study showed that on large TiO_2 crystallite size, the SMSI effect may not be detected (Weerachawansak *et al.*, 2008). Moreover, the SMSI effect on Pd/TiO_2 depends on TiO_2 crystal structure (anatase and rutile). It has been reported that reduction by H_2 at lower temperature results in SMSI for anatase titania supported palladium catalyst, but not for rutile titania supported palladium catalyst (Li *et al.*, 2004).

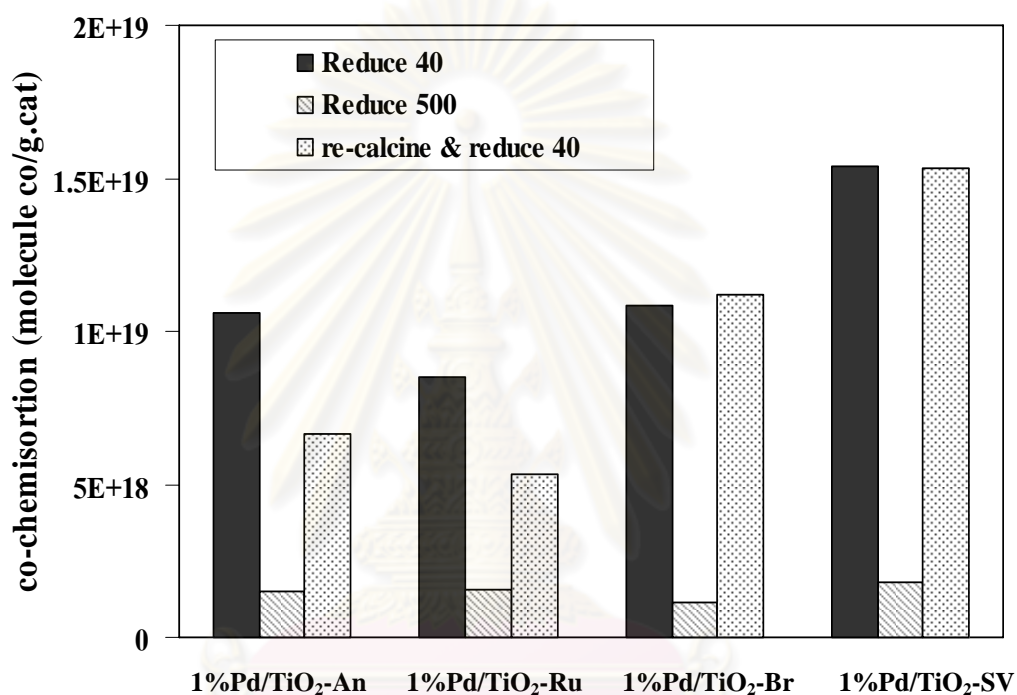


Figure 5.6 The results of SMSI test on 1%Pd/TiO₂ catalysts

ศูนย์วิทยทรัพยากร
จุฬาลงกรณ์มหาวิทยาลัย

5.1.7 Electron Spin Resonance Spectroscopy (ESR)

Electron spin resonance technique is a technique for studying chemical species that have one or more unpaired electrons, such as organic and inorganic free radicals or inorganic complexes possessing a transition metal ion.

The number of defective sites of TiO_2 was determined using electron spin resonance spectroscopy technique and the results are shown in Figure 5.7. The signal of g value less than 2 was assigned to Ti^{3+} ($3d^1$) (Salama *et al.*, 1993). Nakaoka and Nosaka (Nakaoka and Nosaka, 1997) reported six signals of ESR measurement occurring on the surface of titania: (i) $\text{Ti}^{4+}\text{O}^-\text{Ti}^{4+}\text{OH}^-$, (ii) surface Ti^{3+} , (iii) adsorbed oxygen (O^{2-}), (iv) $\text{Ti}^{4+}\text{O}^{2-}\text{Ti}^{4+}\text{O}^{2-}$, (v) inner Ti^{3+} , and (vi) adsorbed water. In this thesis, it was clearly seen that the TiO_2 -Br and TiO_2 -SV exhibited only one signal at g value of 1.997 which can be attributed to Ti^{3+} at the surface. Many Ti^{3+} ESR signals were observed for the TiO_2 -An, indicating that more than one type of Ti^{3+} defects were presented in the sample i.e., surface Ti^{3+} and inner Ti^{3+} . It should be noted that the Ti^{3+} ESR signal was observed only for the anatase TiO_2 . For brookite titania (TiO_2 -Br), it had ESR signal of Ti^{3+} on surface because TiO_2 -Br was mixed phase of brookite and anatase. None of Ti^{3+} ESR signal was observed for TiO_2 -Ru. It was suggested that Ti^{4+} in the rutile TiO_2 is difficult to be reduced to Ti^{3+} . As rutile titania was more thermodynamically and structurally stable than anatase titania, the Ti^{3+} ions fixed in the surface lattice of anatase TiO_2 was easier to diffuse to the surface than one in the surface lattice of rutile TiO_2 . Besides, ESR signal of Ti^{3+} promoted strong metal–support interaction (SMSI) in anatase titania supported palladium (Li *et al.*, 2003). The intensity of the Ti^{3+} signal was highest for TiO_2 -SV suggesting that this preparation method produces the highest amount of defects on the TiO_2 (Panpranot *et al.*, 2006).

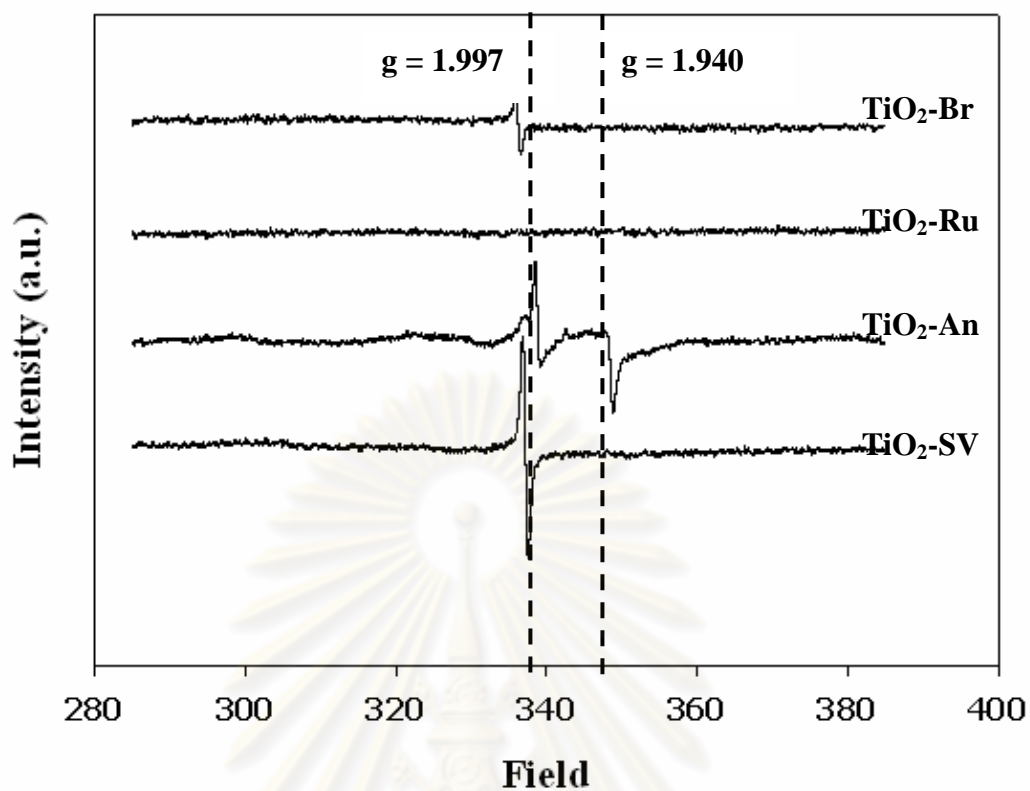


Figure 5.7 ESR spectra of TiO₂

ศูนย์วิทยทรัพยากร
จุฬาลงกรณ์มหาวิทยาลัย

5.2 Reaction study in phenylacetylene hydrogenation

Reaction study of the catalysts in liquid phase semihydrogenation of phenylacetylene was determined in terms of phenylacetylene conversion and selectivity towards styrene. Phenylacetylene conversion is defined as moles of phenylacetylene consumed with respect to phenylacetylene in the feed. Selectivity is the ratio of the mole of styrene (desired product) and the total mole of products (styrene and ethylbenzene). Ideally, there should be one phenylacetylene molecule converted to styrene for every hydrogen molecule consumed, or 100% selectivity, since all of the phenylacetylene is converted into styrene. In actual practice, some hydrogen will always be consumed in side reaction of styrene converted to ethylbenzene.

5.2.1 Comparison of organic solvent and scCO₂ in semihydrogenation of phenylacetylene on 1%Pd/TiO₂-An catalyst.

The effects of supercritical CO₂ and organic solvent on phenylacetylene hydrogenation over 1%Pd/TiO₂-An catalysts were studied at a constant temperature of 313 K and hydrogen pressure of 1 MPa. Table 5.5 shows phenylacetylene conversion and styrene selectivity for 1%Pd/TiO₂-An R40 and R500 in scCO₂, ethanol, solventless condition, and the mixture of scCO₂ and ethanol. It was observed that %conversion increased in the order scCO₂>solventless>ethanol>scCO₂+ethanol with little effect on selectivity to styrene. In hydrogenation reaction, H₂ solubility in common organic solvents is usually low. Dissolution of scCO₂ enhanced H₂ solubility thus hydrogenation activity increased. On the other hand, the use of mixture between scCO₂ and ethanol led to lower catalytic activity due probably to the formation of a biphasic reaction mixture. Similar results were also observed by Grunwaldt *et al.* (Grunwaldt *et al.*, 2005) for the use of toluene-modified scCO₂ in oxidation reaction. In any reaction medium, the 1%Pd/TiO₂-An catalyst reduced at 40°C showed higher hydrogenation activity than that reduced at 500°C. The lower activity of the catalysts reduced at 500°C was probably due to metal sintering and lower Pd dispersion.

Table 5.5 Semihydrogenation of phenylacetylene on 1%Pd/TiO₂-An catalysts

Catalyst	solventless		Ethanol ^a		scCO ₂ ^b		scCO ₂ +Ethanol	
	%Con.	%Sel.	%Con.	%Sel.	%Con.	%Sel.	%Con.	%Sel.
1%Pd/TiO ₂ -R40	60	97	57	96	71	92	43	94
1%Pd/TiO ₂ -R500	41	97	46	98	58	96	40	96

Reaction conditions: phenylacetylene = 1 ml, catalyst = 0.005 g, reaction time = 1 hr,

^a ethanol = 9 ml, ^b P_{CO_2} = 10 MPa, %Con. = %Phenylacetylene Conversion and %Sel.

= %Styrene Selectivity

5.2.2 Influence of CO₂ pressure and reaction time on the catalytic behavior of different 1%Pd/TiO₂ catalysts in semihydrogenation of phenylacetylene.

The reaction study of 1%Pd/TiO₂-An catalysts was evaluated in the liquid-phase semihydrogenation of phenylacetylene to styrene in a batch-type stainless steel reactor. The reaction was carried out in scCO₂ at 313 K and H₂ pressures 1 MPa. The substrate (phenylacetylene) was 1 ml and amount of catalysts was 0.005 g.

The effect of CO₂ pressure on the phenylacetylene conversion and styrene selectivity for 1%Pd/TiO₂-An R40 and R500 is shown in Figure 5.8. It was evident that phenylacetylene conversion for both 1%Pd/TiO₂-An catalysts increased with increasing CO₂ pressure from 6 to 14 MPa. There was no effect of CO₂ pressure on styrene selectivity for both catalysts (styrene selectivity > 80%). The metal particle size of these two catalysts was quite different and larger metal particles were seen to exist on the catalyst reduced at 500°C (see Table 5.4). The lower activity of 1%Pd/TiO₂-An R500 was probably due to lower amount of active Pd metal on the surface as a result of metal sintering. Furthermore, CO₂ pressure affected most of its properties. It was known that an organic liquid may expand under pressurized CO₂, which results from dissolution of CO₂ and/or other gaseous species into the liquid (Arai *et al.*, 2004). On the other hand, if the liquid substrate is easy to dissolve into the CO₂ gas phase at increasing CO₂ pressure, such dissolution reduced the volume of liquid phase and exceeded the volume expansion due to the dissolution of CO₂ and H₂ (Zhao *et al.*, 2006).

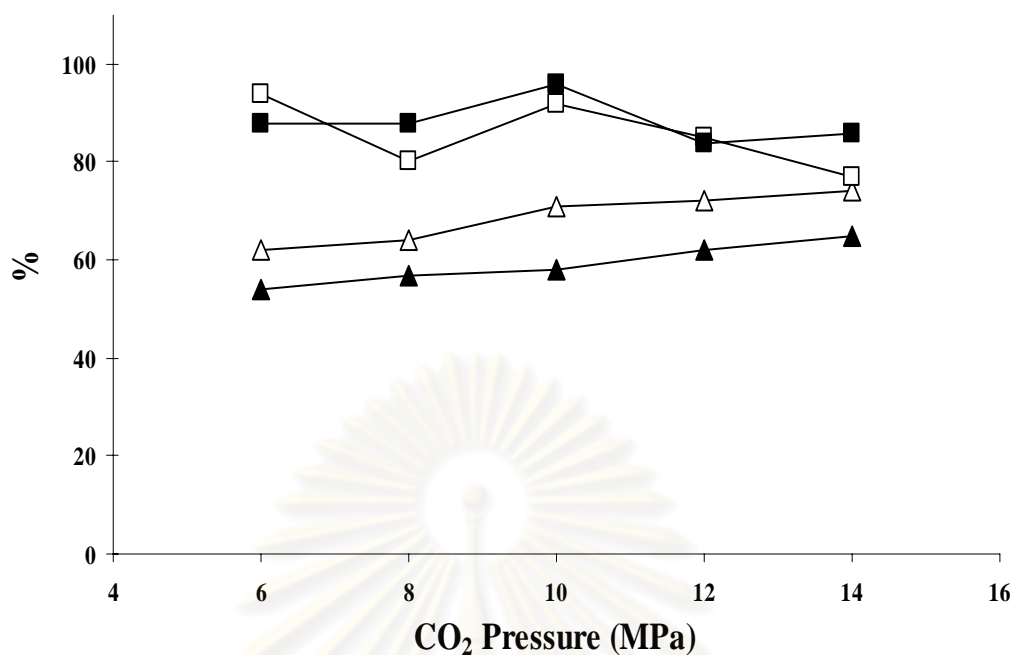


Figure 5.8 Influence of CO₂ pressure on semihydrogenation of phenylacetylene on 1%Pd/TiO₂-An catalyst.

△ = %Phenylacetylene Conversion and □ = %Styrene Selectivity

(Open symbol: R 40, Close symbol: R 500)

The changes of total conversion and selectivity with time for the semihydrogenation of phenylacetylene over 0.005 g of 1%Pd/TiO₂-An in 10 MPa of carbon dioxide at 313 K are shown in Figure 5.9. It is shown that phenylacetylene conversion for both 1%Pd/TiO₂-An catalysts increased with increasing reaction time. In the presence of 1%Pd/TiO₂-An catalyst reduced at 40°C, the conversion of phenylacetylene was also completed (~100%) at 120 min. In contrast, the conversion of catalysts reduced at 500°C at that time was approximately 65%. There was no styrene selectivity (~90%) change for catalysts reduced at 500°C when reaction time increased. For 1%Pd/TiO₂-An catalyst reduced at 40°C, when the reaction time changed from 30 to 120 min the selectivity decreased from 90 to 50%. The hydrogenation of styrene to ethylbenzene occurred when the concentration of phenylacetylene was sufficiently low indicating a slower parallel reaction pathway for the direct hydrogenation of phenylacetylene to ethylbenzene (Jackson and Shaw., 1996).

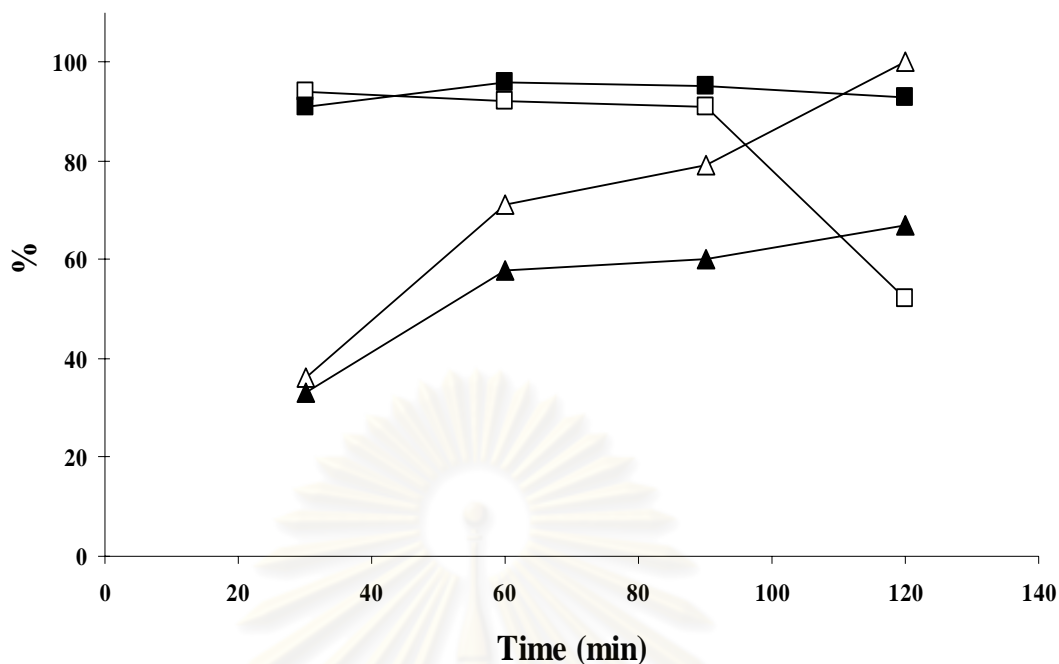


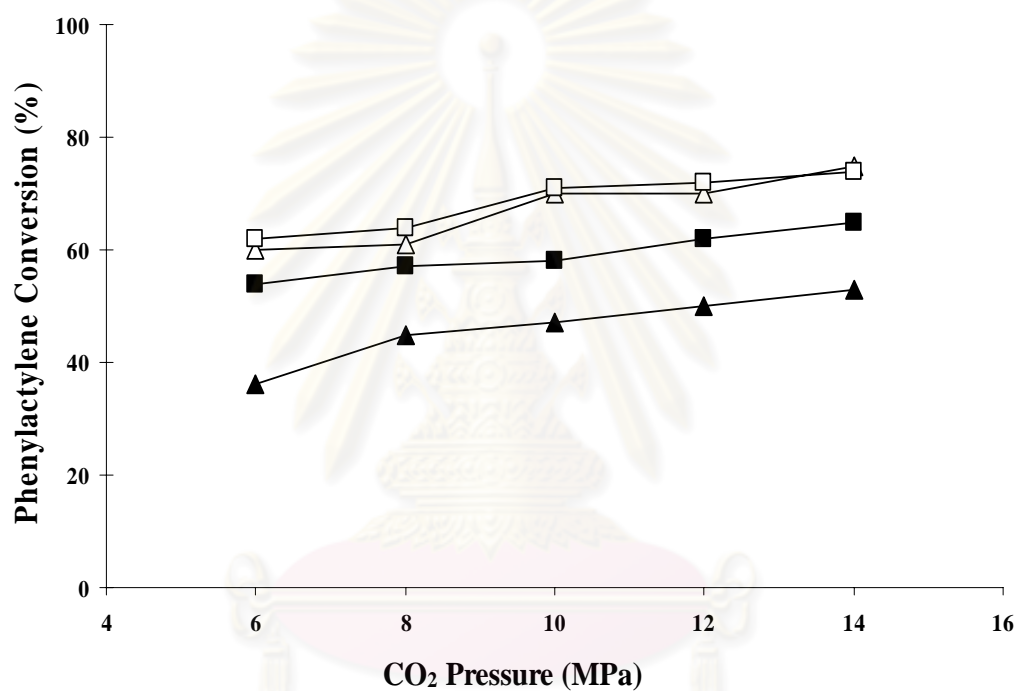
Figure 5.9 Influence of reaction time on semihydrogenation of phenylacetylene

Δ = % Phenylacetylene Conversion and \square = % Styrene Selectivity

(Open symbol: R 40, Close symbol: R 500)

The effect of CO_2 pressure on the catalytic behavior of 1%Pd catalysts supported on TiO_2 phases (anatase and brookite) was also studied and the results are shown in Figure 5.10. The same trend is seen with these catalysts: phenylacetylene conversion for both catalysts increased with increasing CO_2 pressure. The phenylacetylene conversion of both catalysts when reduced at 40°C were higher than those reduced at 500°C . For the catalysts reduced at 40°C , phenylacetylene conversion was similar due probably to the similar amounts of active Pd metal on the surface. However, the catalysts reduced at 500°C , 1%Pd/ TiO_2 -An showed higher conversion of phenylacetylene than 1%Pd/ TiO_2 -Br. The lower activity of 1%Pd/ TiO_2 -Br R500 was probably due to phase transformation of TiO_2 support from brookite to rutile phase (see Table 5.1). It has been shown that anatase TiO_2 support catalysts exhibited higher activity than rutile supported one, For example, Rao and coworker reported that anatase supported ceria catalyst exhibited higher ammoxidation activities than rutile supported ceria catalyst and pure ceria (Rao *et al.*, 1997). Besides, the BET surface areas of 1%Pd/ TiO_2 -Br catalysts rapidly decreased after reduction at 500°C . Such results indicate that pore blockage or destruction of the TiO_2

pore structure occurred during high temperature treatment. For styrene selectivity, there was no effect of CO₂ pressure on styrene selectivity for both catalysts (styrene selectivity > 80%)



ศูนย์วิทยทรัพยากร
จุฬาลงกรณ์มหาวิทยาลัย

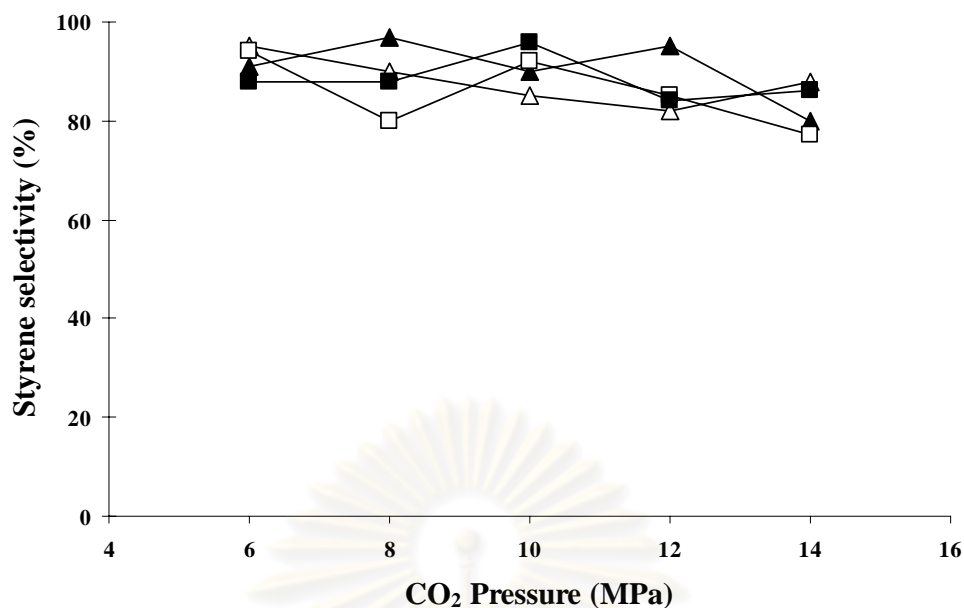


Figure 5.10 Influence of CO₂ pressure on semihydrogenation of phenylacetylene on 1%Pd/TiO₂-An and 1%Pd/TiO₂-Br catalysts.

Reaction condition: phenylacetylene = 1 ml, catalyst = 0.005 g, P_{H_2} = 1 MPa, reaction time = 1 hr, Temperature = 313 K.

Δ = 1%Pd/TiO₂-Br and \square = 1%Pd/TiO₂-An

(Open symbol: R 40, Close symbol: R 500)

In the following section, the catalysts with similar TiO₂ phase (anatase) 1%Pd/TiO₂-An and 1%Pd/TiO₂-SV were selected for comparison. The two catalysts possessed different TiO₂ crystallite sizes. The 1%Pd/TiO₂-SV exhibited the SMSI effect whereas the 1%Pd/TiO₂-An did not (see SMSI test in 5.1.6). The performance of the 1%Pd/TiO₂-An and 1%Pd/TiO₂-SV catalysts in semihydrogenation of phenylacetylene under scCO₂ are shown in Figure 5.11. As can be observed, both catalysts exhibited high styrene selectivity (>85%) for phenylacetylene conversion less than 80%. The selectivity of styrene significantly dropped to 25-65% when conversion of phenylacetylene reached 100% for all catalysts except 1%Pd/TiO₂-SV reduced at 500°C that retained its high styrene selectivity > 70%. Such results suggest that the strong metal-support interaction on 1%Pd/TiO₂-SV catalyst produced great beneficial effect on the catalyst performance. The presence of SMSI effect may result in an inhibition of the adsorption of the product styrene on the 1%Pd/TiO₂-SV hence high styrene selectivity was obtained (Panpranot *et al.*, 2009). The SMSI effect could reasonably explain our results. The titania support was partly reduced and suboxide

phase migrated onto the metal particle. Then, part of the metal surface partially covered by TiO_x was blocked (Haller and Resasco, 1989). This led to a decrease of interaction between product and metal surface. Thus, the product was easy to take off from metal surface. The 1%Pd/ TiO_2 -An reduced at 500°C exhibited the lowest styrene selectivity at complete conversion of phenylacetylene. It was suggest that styrene and/or phenylacetylene were hydrogenated to ethylbenzene. Moreover, the catalyst was probably deactivated by sintering during reduction at high temperature.

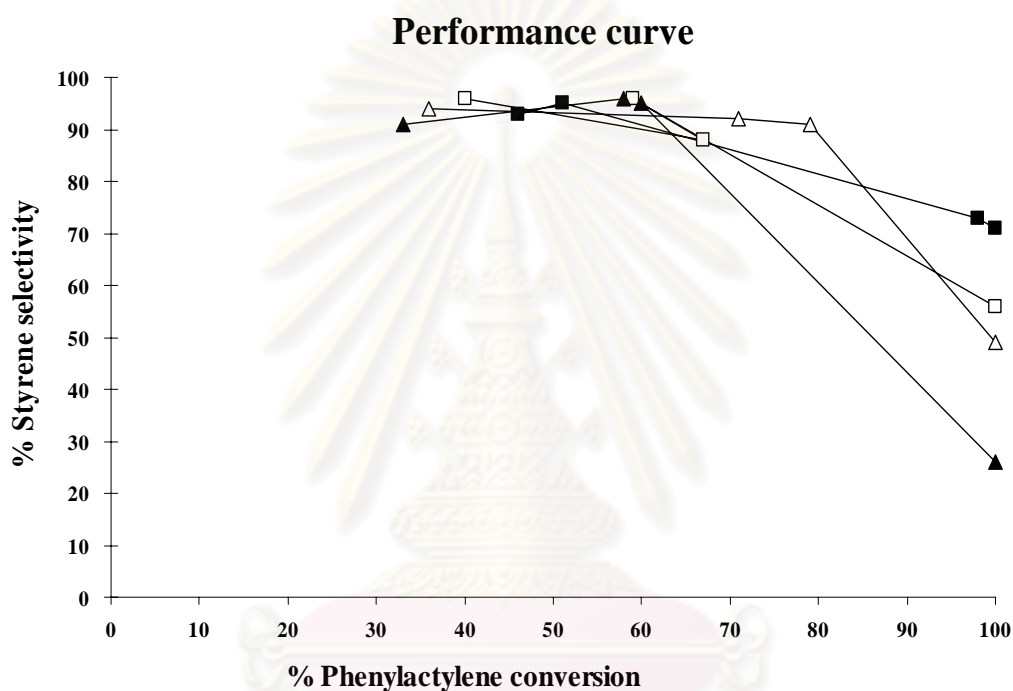


Figure 5.11 Performance curve of 1%Pd/ TiO_2 An and SV

Reaction condition: phenylacetylene = 1 ml, catalyst = 0.005 g, P_{H_2} = 1-2 MPa, P_{CO_2} = 10 Mpa, Temperature = 313 K, reaction time 30-60 min

Δ = 1%Pd/ TiO_2 -An and \square = 1%Pd/ TiO_2 -SV

(Open symbol: R 40, Close symbol: R 500)

5.2.3 Effect of Pd⁰ metal particle size on semihydrogenation of phenylacetylene in organic solvent and scCO₂

The semihydrogenation of phenylacetylene with different Pd/TiO₂ catalysts reduced at 40°C was examined in scCO₂ and ethanol under different conditions. The variation of phenylacetylene conversion and styrene selectivity with Pd⁰ metal particle size for the two reaction systems are shown in Figure 5.12. The Pd⁰ metal particle sizes were calculated from the CO chemisorption results of the catalysts reduced at 40°C (see Table 5.4). While the product selectivity in ethanol did not change so much with the size of Pd⁰ particles, the conversion of phenylacetylene increased from 9 to 24% with a change in Pd⁰ particle size from 4.2 to 6.7 nm. In scCO₂, both the total conversion and selectivity did not change much with increasing in the Pd⁰ particle size. Thus, we can say that no effect of Pd particle size on specific activity in scCO₂. On the other hand, the conversion increased with an increase in the Pd⁰ particle size in organic solvent (ethanol). We can probably say that the reaction is structure sensitive in ethanol. Ikushima et al. studied hydrogenation of nitrobenzene (NB) with Pt/C catalysts in supercritical carbon dioxide (scCO₂) and ethanol. They reported that the overall hydrogenation of NB is not structure sensitive in scCO₂, while it is structure sensitive in ethanol in which turnover frequency tends to decrease with an increase in the degree of Pt dispersion (Ikushima *et al.*, 2004)

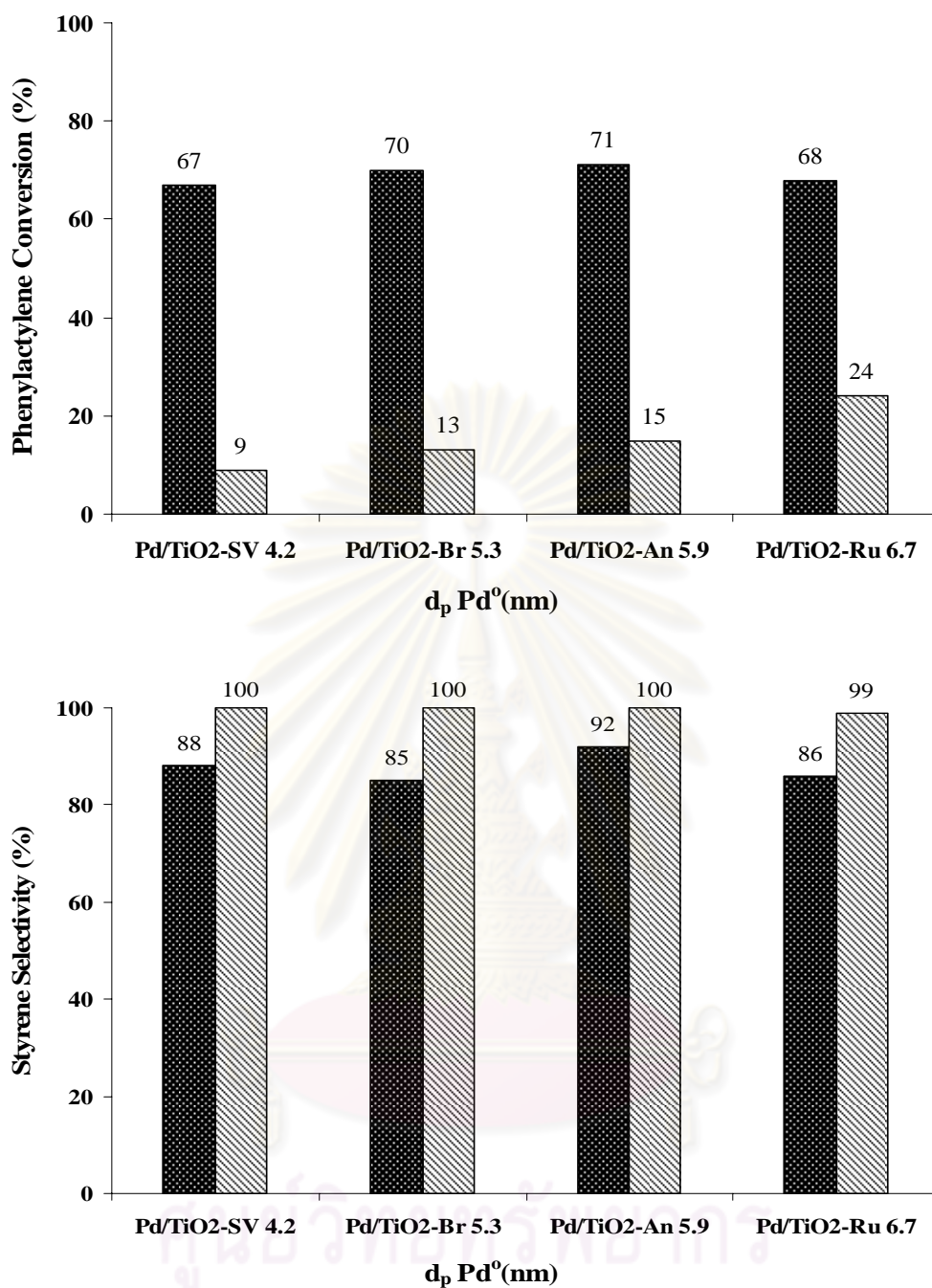


Figure 5.12 Influence of metal particle size on the overall conversion of phenylacetylene and selectivity to styrene for 1%Pd/TiO₂-R40 in organic solvent and scCO₂: ■ = scCO₂, ▨ = Ethanol

Reaction conditions: ■ phenylacetylene = 1 ml, CO₂ = 10 MPa, catalyst = 0.005 g, P_{H_2} = 1 MPa, reaction time = 1 hr, Temperature = 313 K.
 ▨ phenylacetylene = 1 ml, Ethanol = 9 ml, catalyst = 0.05 g, P_{H_2} = 1 bar, reaction time = 10 min, Temperature = 303 K.

The turnover frequencies (TOFs) were determined based on the number of palladium sites measured by irreversible CO or H₂ chemisorption. Figure 5.13 shows TOF versus Pd⁰ metal particle size. As can be observed, the TOF increased with increasing metal particle size so the reaction was structure sensitive. A number of previous studies (see Table 5.7) have reported that palladium with larger particle size was more active in selective hydrogenation than smaller ones. However, there is probably a limit value of metal particle size for enhancing catalytic activity of Pd⁰ metal particle in this reaction. Kiwi-Minsker et al. studied selective hydrogenation of acetylene with CNF/SMF supported palladium. They reported that antipathetic size dependence of TOF disappeared at particle size bigger than 11 nm. Initial selectivity to ethylene was found to be size-independent. The deactivation due to coke deposition was faster for smaller particles (Kiwi-Minsker *et al.*, 2008).

Table 5.6 Catalytic activity of different 1%Pd/TiO₂ catalysts in semihydrogenation of phenylacetylene in ethanol at 303 K

Catalyst	Phenylacetylene Conversion (%)	Styrene Selectivity (%)	TOFs (s ⁻¹)
1%Pd/TiO ₂ -An R40	15	100	2.7
1%Pd/TiO ₂ -An R500	20	100	25
1%Pd/TiO ₂ -Ru R40	24	99	5.2
1%Pd/TiO ₂ -Ru R500	16	100	19.9
1%Pd/TiO ₂ -Br R40	13	100	2.2
1%Pd/TiO ₂ -Br R500	10	100	14.8
1%Pd/TiO ₂ -SV R40	9	100	1.1
1%Pd/TiO ₂ -SV R500	14	100	14.4

Reaction condition: Phenylacetylene = 1 ml, Ethanol = 9 ml, catalyst = 0.05 g,

P_{H_2} = 1 bar, reaction time = 10 min, Temperature = 303 K.

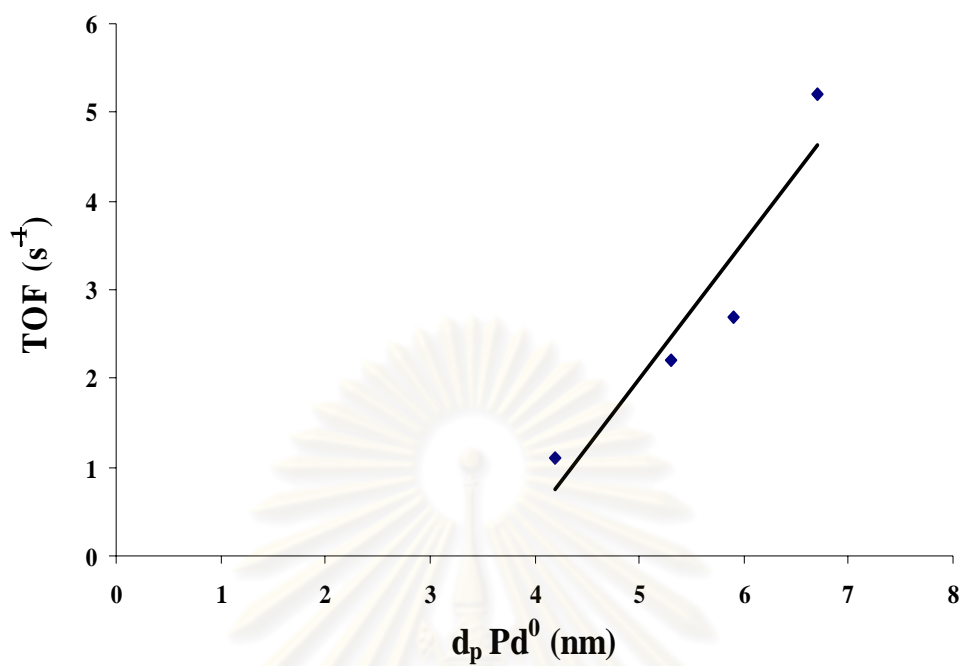


Figure 5.13 Plot TOF against metal particle size for semihydrogenation of phenylacetylene in ethanol

ศูนย์วิทยทรัพยากร
จุฬาลงกรณ์มหาวิทยาลัย

Table 5.7 Previous studies reporting the effect of Pd⁰ metal particle size in selective hydrogenation reaction in which larger Pd⁰ particle size was found to be more activity.

Reaction	d _p Pd ⁰ (nm)	Ref.
<i>cis,trans,trans</i> -1,5,9-cyclododecatriene	1.5-10	Cabiac et al.,2006
1-hexyne hydrogenation	6-11	Semagina et al.,2007
Semi-hydrogenation of phenylacetylene	3-12	Panpranot et al.,2007
Semi-hydrogenation of phenylacetylene	2-8	Dominguez-Dominguez et al.,2008

ศูนย์วิทยทรัพยากร
จุฬาลงกรณ์มหาวิทยาลัย

CHAPTER VI

CONCLUSIONS AND RECOMMENDATIONS

In this chapter, section 6.1 provides the conclusions obtained from the experimental results of liquid phase semihydrogenation of phenylacetylene to styrene on Pd/TiO₂ in supercritical carbon dioxide. Additionally, recommendations for further study are given in section 6.2.

6.1 Conclusions

1. Liquid phase semihydrogenation of phenylacetylene on Pd/TiO₂ was enhanced when performed in high pressure CO₂ but those carried out in organic solvent was not change. On the other hand, the mixture of ethanol and scCO₂ may lead to a biphasic reaction mixture so that lower catalytic activity was obtained.

2. The Pd particle size did not affect specific activity for semihydrogenation of phenylacetylene in scCO₂ but in ethanol, the reaction appeared to be structure sensitive since the TOF increase with an increase in Pd particles size.

3. Reaction at high temperature (500°C) for An 500 resulted in Pd metal sintering while for Br 500 resulted in TiO₂ phase change. Both cases led to lower catalyst performance compared to those reduced at 40°C.

However, for TiO₂-SV the catalyst exhibited SMSI effect which improved catalyst performance although the reaction was carried out in scCO₂.

6.2 Recommendations

1. The mechanism for deactivation of metal catalyst due to metal leaching and metal sintering during liquid phase semihydrogenation of phenylacetylene in scCO₂ should be studied.
2. Another experiment of activity and selectivity of Pd on rutile titania when reduced at 500°C in this reaction. And furthermore study about effect of temperature of overall reaction.
3. The support should be treated at reduced temperature before impregnated with Pd.



REFERENCES

- Ali, S. H., and Goodwin, J. G., Jr. SSITKA Investigation of Palladium Precursor and Support Effects on CO Hydrogenation over Supported Pd Catalysts. J. Catal. 176(1998):3-13.
- Anderson, A. B., and Onwood, D. P. Why carbon monoxide is stable lying down on a negatively charged Ru(001) surface but not on Pt (111). Surface Science Letters. 154(1985):L261-L267.
- Bhanage, B.M., Ikushima, Y., Shirai, M., and Arai, M. The selective formation of unsaturated alcohols by hydrogenation of α,β -unsaturated aldehydes in supercritical carbon dioxide using unpromoted Pt/Al₂O₃ catalyst. Catal. Letters. 62(1999): 175-177.
- Caravati, M., Grunwaldt, J.D., and Baiker, A. Solvent- modified supercritical CO₂:A beneficial medium for heterogeneously catalyzed oxidation reaction. Applied Catalysis A. 298(2005):50-56.
- Cabiac, A., Delahay, G., Durand, R., Trens, P., Ple'e, D., Medevielle, A., and Coq, B. The influence of textural and structural properties of Pd/carbon on the hydrogenation of cis,trans,trans-1,5,9-cyclododecatriene. App Catal A. 318(2007): 17-21.
- Chatterjee, M., Chatterjee, A., and Ikushima, Y. Pd-catalyzed completely selective hydrogenation of conjugated and isolated CNC of citral (3,7-dimethyl-2, 6-octadienal) in supercritical carbon dioxide. Green Cheem. 6(2004): 114-118.
- Chung-Sik, K., Moonb, B.K., Parka, J.H., Chungc, S.T. and Sond, S.M. Synthesis of nanocrystalline TiO₂ in toluene by a solvothermal route. Jol. Crystal Growth. 254(2003): 405-410.
- Christopher, A.N., Daniel, E.S, Sujaree, K., Courtney, J.K., Daniel, H.M., John, P.R., Jamie, L.W., Radhika, B., and Buetrand, I.L. Photocatalytic study of polymorphic titania synthesized by ambient condition sol process. Cat. Lett. (2007)
- Dominguez-Dominguez, S., Berenguer-Murcia, A., Pradhan, B.K., Linares-Solano, A., and Cazorla-Amoro, D. Semihydrogenation of phenylacetylene catalyzed

- by palladium nanoparticles supported on carbon materials. J. Phys. Chem. 112 (2008): 3827-3834.
- Dominguez-Dominguez, S., Berenguer-Murcia, A., Pradhan, B.K., Linares-Solano, A., and Cazorla-Amoro, D. Inorganic materials as supports for palladium nanoparticles: Application in the semi-hydrogenation of phenylacetylene. Jal. Catal. 257(2008): 87-95.
- Huang, X., Wilhite, B., McCready, M. J., Varma, A. Phenylacetylene hydrogenation in a three-phase catalytic packed-bed reactor: experiments and model. Chem. Eng. Sci. 58 (2003): 3465 – 3471.
- Kang, M., Lee, S. Y., Chung, C.H., Cho, S. M., Han, G. Y., Kim, B.W., Yoon, K. J. Characterization of a TiO₂ photocatalyst synthesized by the solvothermal method and its catalytic performance for CHCl₃ decomposition. J. Photochem. Photobiol. A 144 (2001): 185–191.
- Kongsuebchart, W., Prasertdam, P., Panpranot, J., Sirisuk, A., Supphasrirongjaroen, P., and Satayaprasert, C. Effect of crystallite size on the surface defect of nano-TiO₂ prepared via solvothermal synthesis. Jol. Crystal Growth. 297 (2006): 234-238.
- Li, Y., Xu, B., Fan, Y., Feng, N., Qiu, A., He, J. M. J., Yang H., and Chen, Y. The effect of titania polymorph on the strong metal-support interaction of Pd/TiO₂ catalysts and their application in the liquid phase selective hydrogenation of long chain alkadienes. J. Mol. Catal.A. 216(2004): 107–114.
- Liu., R., Zhao, F., Fujita, S.I., and Arai, M. Selective hydrogenation of citral with transition metal complexes in supercritical carbon dioxide. Applied Catalysis A. 316(2007): 127-133.
- Mahata, N., and Vishwanathan, V. Influence of palladium precursors on structural properties and phenol hydrogenation characteristics of supported palladium catalysts. J.Catal. 196(2000): 262-270.
- Musolino, M.G., Apa, G., Donato, A., Pietropaolo, A., and Frusteri, F. Supported palladium catalysts for the selective conversion of cis-2-butene-1,4-diol to 2-hydroxytetrahydrofuran: effect of metal particle size and support. Applied Catalysis A. 325(2007): 112–120.

- Panpranot, J., Phandinthong, K., Praserttham, P., Hasegawa, M., Fujita, S., and Arai, M. A comparative study of liquid-phase hydrogenation on Pd/SiO₂ in organic solvents and under pressurized carbon dioxide: Activity change and metal leaching/sintering. J. Mol. Catal. A. 253(2006): 20–24.
- Panpranot, J., Phandinthong, K., Sirikajorn, T., Arai, M., and Praserttham, P. Impact of palladium silicide formation on the catalytic properties of Pd/SiO₂ catalysts in liquid-phase semihydrogenation of phenylacetylene. Jol. Mol. Catal. A:Chem. 261(2007):29-35.
- Rao, P.K., Rama Rao, K.S., Masthan, S.K., Narayana, K.V., Rajiah, T., and Rao, V.V. Highly active titania supported ceria catalysts for ammoxidation of picolines. App Catal A. 163(1997):123-127.
- Ruta, M., Semagina, N., and Kiwi-Minsker, L. Monodispersed Pd Nanoparticles for acetylene selective hydrogenation: particle size and support effects. J. Phys. Chem. C. 112(2008): 13635-13641.
- Sales, E.A., Bugli, G., Ensuque, A., Mendes, M. J. and Bozon-Verduraz, F. Phys. Chem. Chem. Phys. 1(1999): 491.
- Semagina, N., Renken, A., and Kiwi-Minsker, L. Palladium nanoparticle size effect in 1-hexyne selective hydrogenation. J. Phys. Chem. 111(2007): 13933-13937.
- Singh, U.K. and Vannice, M.A. Liquid-Phase citral hydrogenation over SiO₂-Supported group VIII metals. Jal. Catal. 199(2001): 73-84.
- Tauster, S.J., Fung, S.C., Garten, R.L. Strong Metal-Support Interactions Group 8 Noble Metals Supported on TiO₂. J. Ame.Chem.Soc. (1978): 170-174.
- Tschan, R., Wandeler, R., Schneider, M., Schubert, M.S., and Baiker, A. Continuous semihydrogenation of phenylacetylene over amorphous Pd₈₁Si₁₉ Alloy in “Supercritical” Carbon Dioxide: Relation between catalytic performance and phase behavior. Jol. Catal. 204(2001): 219-229.
- Vergunst, T., Kapteijn, F., and Moulijn, J.A. Optimization of geometric properties of a monolithic catalyst for the selective hydrogenation of phenylacetylene. Ind. Eng. Chem. Res. 40(2001): 2801-2809.

- Weerachawansak, P., Prasertthdam, P., Arai, M., and Panpranot, J. A comparative study of strong metal-support interaction and catalytic behavior of Pd catalysts supported on micron- and nano-sized TiO₂ in liquid-phase selective hydrogenation of phenylacetylene. Jol. Mol. Catal. A. 279(2008):133-139.
- Weerachawansak, P., Mekasuwandumrong, O., Prasertthdam, P., Fujita, S.I., Arai, M., and Panpranot, J. Effect of strong metal-support interaction on the catalytic performance of Pd/TiO₂ in liquid-phase semihydrogenation of phenylacetylene. Jol. Catal. 262(2009):199-205.
- Zhang, H., and Benfield, J. Understanding polymorphic phase transformation behavior during growth of nanocrystalline aggregates: Insights from TiO₂. Jol. Phys. Chem B. 104(15): 3481-3487.
- Zhao, F., Ikushima, Y., Chatterjee, M., Sato, O., and Arai, M. Hydrogenation of an α , β -unsaturated aldehyde catalyzed with ruthenium complexes with different fluorinated phosphine compounds in supercritical carbon dioxide and conventional organic solvents. Jal. Supercritical Fluid. 27(2003): 65-72.
- Zhao, F., Ikushima, Y., and Arai, M. Hydrogenation of nitrobenzene with supported platinum catalysts in supercritical carbon dioxide: effect of pressure, solvent, and metal particle size. Jol Catal. 224(2004): 479-483.
- Zhao, F., Fujita, S.I., Sun, J., Ikushima, Y., and Arai, M. Carbon dioxide-expanded liquid substrate phase: an effective medium for selective hydrogenation of cinnamaldehyde to cinnamyl alcohol. Chem Commun. (2004): 2326-2327.



APPENDICES

ศูนย์วิทยทรัพยากร
จุฬาลงกรณ์มหาวิทยาลัย

APPENDIX A

CALCULATION FOR CATALYST PREPARATION

Preparation of 1%Pd/TiO₂ catalysts by the incipient wetness impregnation method are shown as follows:

Reagent: - Palladium (II) nitrate hexahydrate (Pd (NO₃)₂ · 6H₂O)
 Molecular weight = 338.52
 - Support: Titania [TiO₂]

Example Calculation for the preparation of 1%Pd/TiO₂

Based on 100 g of catalyst used, the composition of the catalyst will be as follows:

Palladium	=	1 g	
Titania	=	100-1	= 99 g

For 3 g of titania

Palladium required	=	3×(1/99)	=	0.0303 g
--------------------	---	----------	---	----------

Palladium 0.0303 g was prepared from Pd (NO₃)₂ · 6H₂O and molecular weight of Pd is 106.42

$$\begin{aligned} \text{Pd (NO}_3)_2 \cdot 6\text{H}_2\text{O required} &= \frac{\text{MW of Pd(NO}_3)_2 \cdot 6\text{H}_2\text{O} \times \text{palladium required}}{\text{MW of Pd}} \\ &= (338.52/106.42) \times 0.0303 = 0.0964 \text{ g} \end{aligned}$$

Since the pore volume of the titania support is 0.4 ml/g. Thus, the total volume of impregnation solution which must be used is 1.2 ml for titania by the requirement of incipient wetness impregnation method, the de-ionized water is added until equal pore volume for dissolve Palladium (II) nitrate hexahydrate.

APPENDIX B

CALCULATION OF THE CRYSTALLITE SIZE

Calculation of the crystallite size by Debye-Scherrer equation

The crystallite size was calculated from the half-height width of the diffraction peak of XRD pattern using the Debye-Scherrer equation.

From Scherrer equation:

$$D = \frac{K\lambda}{\beta \cos \theta} \quad (\text{B.1})$$

where D = Crystallite size, Å
 K = Crystallite-shape factor = 0.9
 λ = X-ray wavelength, 1.5418 Å for CuK α
 θ = Observed peak angle, degree
 β = X-ray diffraction broadening, radian

The X-ray diffraction broadening (β) is the pure width of a powder diffraction free from all broadening due to the experimental equipment. α -Alumina is used as a standard sample to observe the instrumental broadening since its crystallite size is larger than 2000 Å. The X-ray diffraction broadening (β) can be obtained by using Warren's formula.

From Warren's formula:

$$\beta = \sqrt{B_M^2 - B_S^2} \quad (\text{B.2})$$

Where B_M = The measured peak width in radians at half peak height.
 B_S = The corresponding width of the standard material.

Example: Calculation of the crystallite size of TiO₂-micron

$$\begin{aligned} \text{The half-height width of peak} &= 0.23^\circ \text{ (from Figure B.1)} \\ &= (2\pi \times 0.23)/360 \\ &= 0.00401 \text{ radian} \end{aligned}$$

The corresponding half-height width of peak of α -alumina = 0.00383 radian

$$\begin{aligned} \text{The pure width} &= \sqrt{B_M^2 - B_S^2} \\ &= \sqrt{0.00401^2 - 0.00383^2} \\ &= 0.0012 \text{ radian} \end{aligned}$$

$$\beta = 0.0012 \text{ radian}$$

$$2\theta = 25.28^\circ$$

$$\theta = 12.64^\circ$$

$$\lambda = 1.5418 \text{ \AA}$$

$$\begin{aligned} \text{The crystallite size} &= \frac{0.9 \times 1.5418}{0.0012 \cos 12.64} = 1185.07 \text{ \AA} \\ &= 118.5 \text{ nm} \end{aligned}$$

ศูนย์วิทยทรัพยากร
จุฬาลงกรณ์มหาวิทยาลัย

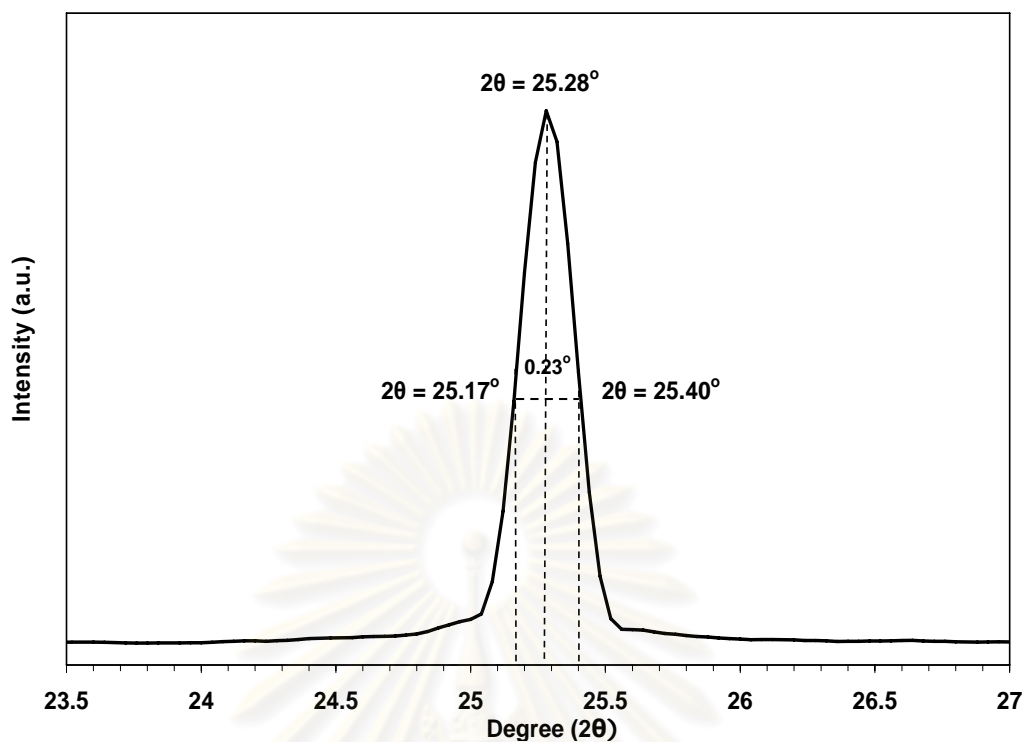


Figure B.1 The measured peak of TiO_2 -micron for calculation the crystallite size.

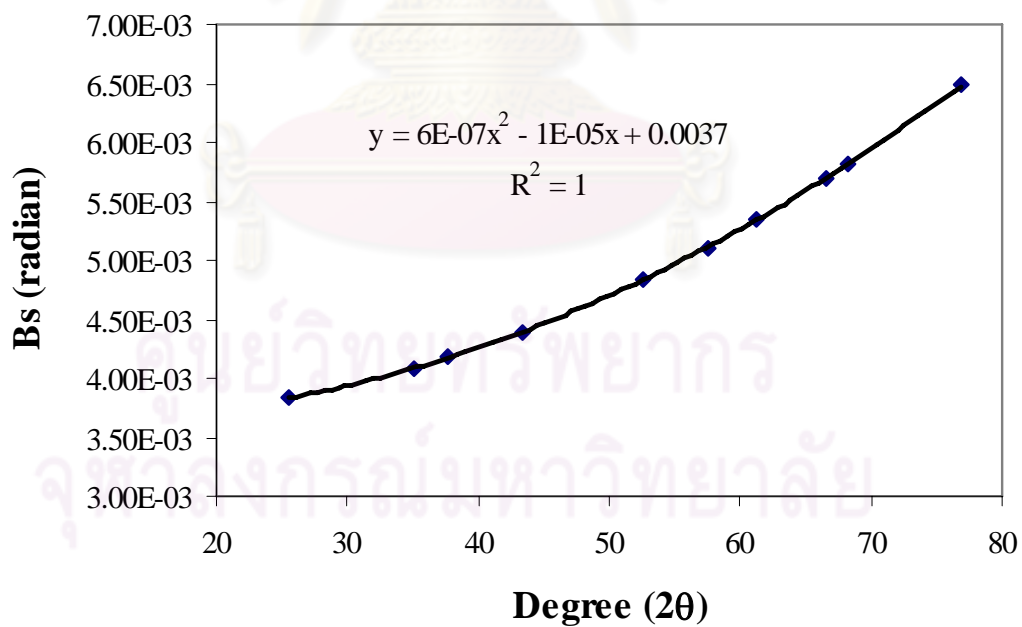


Figure B.2 The plot indicating the value of line broadening due to the equipment. The data were obtained by using α -alumina as standard

APPENDIX C

CALCULATION FOR METAL ACTIVE SITES AND DISPERSION

Calculation of the metal active sites and metal dispersion of the catalyst measured by CO adsorption is as follows:

Calculation of metal active site

Let the weight of catalyst used	= W	g
Integral area of CO peak after adsorption	= A	unit
Integral area of 75 μ l of standard CO peak	= B	unit
Amounts of CO adsorbed on catalyst	= B-A	unit
Volume of CO adsorbed on catalyst	= $75 \times [(B-A)/B]$	μ l
Volume of 1 mole of CO at 30°C	= 24.86×10^6	μ l
Mole of CO adsorbed on catalyst	= $[(B-A)/B] \times [75/24.86 \times 10^6]$	mole
Molecule of CO adsorbed on catalyst	= $[3.02 \times 10^{-6}] \times [6.02 \times 10^{23}] \times [(B-A)/B]$	molecules
Metal active sites	= $1.82 \times 10^{18} \times [(B-A)/B] \times [1/W]$	molecules of CO/g of catalyst

Calculation of %metal dispersion

Definition of % metal dispersion:

Metal dispersion (%)

$$= 100 \times [\text{molecules of Pd from CO adsorption} / \text{molecules of Pd loaded}]$$

In this study, the formula from Chemisorb 2750 Operator's Manual can be used to determine the % metal dispersion as follows:

$$\%D = S_f \times \left[\frac{V_{ads}}{V_g} \right] \times \left[\frac{m.w.}{\%M} \right] \times 100\% \times 100\% \dots \dots \dots (1)$$

Where

%D	=	%metal dispersion
S_f	=	stoichiometry factor, (CO on Pd* =1)
V_{ads}	=	volume adsorbed (cm^3/g)

V_g	=	molar volume of gas at STP = 22414 (cm ³ /mol)
$m.w.$	=	molecular weight of the metal (a.m.u.)
$\%M$	=	%metal loading

Calculation of Average Crystallite Size

Average Crystallite Size of Palladium metal can be calculated base on active metal surface area per gram of metal

$$d_p^{\circ} = \left[\frac{Fg}{p \times MSA_m} \right] \times \left[\frac{m^3}{10^6 cm^3} \right] \times \left[\frac{10^9 nm}{m} \right] \dots \dots \dots (2)$$

Where:

d_p°	=	average crystallite size of Palladium metal
Fg	=	crystallite geometry factor (hemisphere = 6)
p	=	specific gravity of the active metal (Palladium= 12.0 g/cm ³)
MSA_m	=	active metal surface area per gram of metal (m ² /g _{metal})

ศูนย์วิทยทรัพยากร
จุฬาลงกรณ์มหาวิทยาลัย

APPENDIX D

CALCULATION OF PHENYLACTYLENE CONVERSION AND STYRENE SELECTIVITY

The catalytic performance for the phenylacetylene (PA) hydrogenation was evaluated in terms of activity for phenylacetylene conversion and styrene selectivity.

Activity of the catalyst performed in term of phenylacetylene conversion. Phenylacetylene conversion is defined as moles of phenylacetylene converted with respect to phenylacetylene in feed:

$$\text{PA conversion (\%)} = \frac{\text{mole of PA in feed} - \text{mole of PA in product}}{\text{mole of PA in feed}} \times 100$$

Selectivity of product is defined as mole of styrene (ST) formed with respect to mole of styrene and ethylbenzene was obtained:

$$\text{Selectivity of ST (\%)} = \frac{\text{mole of ST formed}}{\text{mole of total product}} \times 100$$

ศูนย์วิทยทรัพยากร
จุฬาลงกรณ์มหาวิทยาลัย

APPENDIX E

CALCULATION OF TURNOVER OF FREQUENCY

Calculation of Turnover frequencies (TOF)

Metal active site = y molecule/g cat.

$$\text{ToF} = \frac{\text{rate}}{\text{(Numbers of active site)}}$$

$$= \frac{\text{molecule substrate converted}}{[\text{g cat.}] [\text{min}]} \left| \frac{[\text{g cat.}] [\text{min}]}{y [\text{active site}]} \right| \frac{[\text{min}]}{[\text{s}]}$$

$$= [\text{s}^{-1}]$$

ศูนย์วิทยทรัพยากร
จุฬาลงกรณ์มหาวิทยาลัย

APPENDIX F

LIST OF PUBLICATIONS

Sukuman Singchai, Joongjai Panpranot, “Liquid-phase semihydrogenation of phenylacetylene on Pd/TiO₂ in supercritical carbon dioxide”, Proceedings of the 2nd SUT Graduate Conference, Nakhon Ratchasima, Thailand, Feb. 21-22, 2009.



ศูนย์วิทยทรัพยากร
จุฬาลงกรณ์มหาวิทยาลัย

VITA

Miss Sukuman Singchai was born in November 3rd, 1984 in Rayong, Thailand. She finished high school from Chonkanyanukoon School, Chonburi in 2003, and received bachelor's degree in Engineering from the department of Chemical Engineering, Faculty of Engineering, Burapha University, Chonburi, Thailand in 2007.



ศูนย์วิทยทรัพยากร
จุฬาลงกรณ์มหาวิทยาลัย